AD-A057 131 PHILIPS LABS BRIARCLIFF MANOR N Y F/G 20/2
GROWTH OF HIGH-QUALITY CESIUM DIDEUTERIUM ARSENATE CRYSTALS.(U)
DEC 76 G M LOIACONO, W N OSBORNE, M DELFINO F33615-75-C-1202
UNCLASSIFIED AFAL-TR-76-215 NL

1 OF 1
ADA
057131

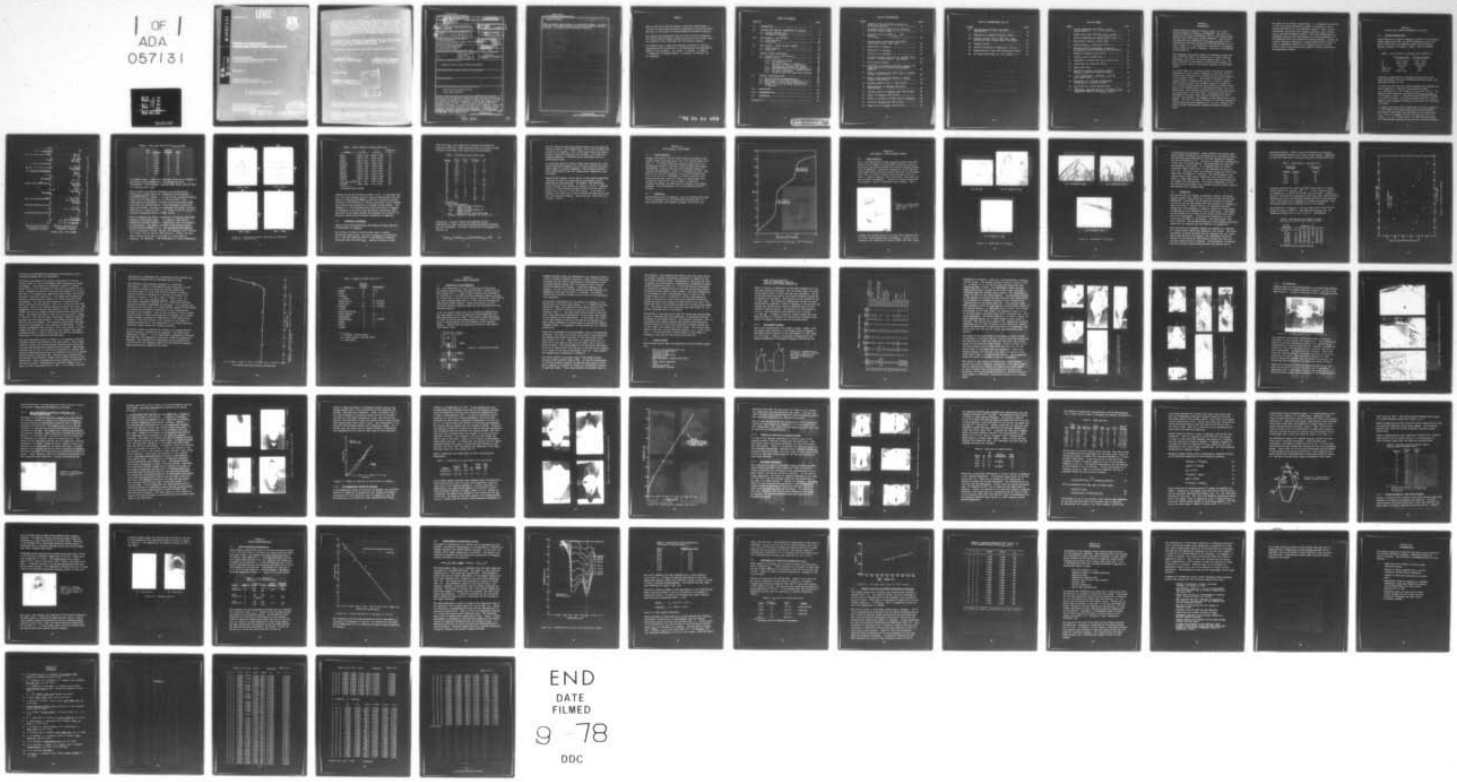

END
DATE
FILMED
9 78
DDC

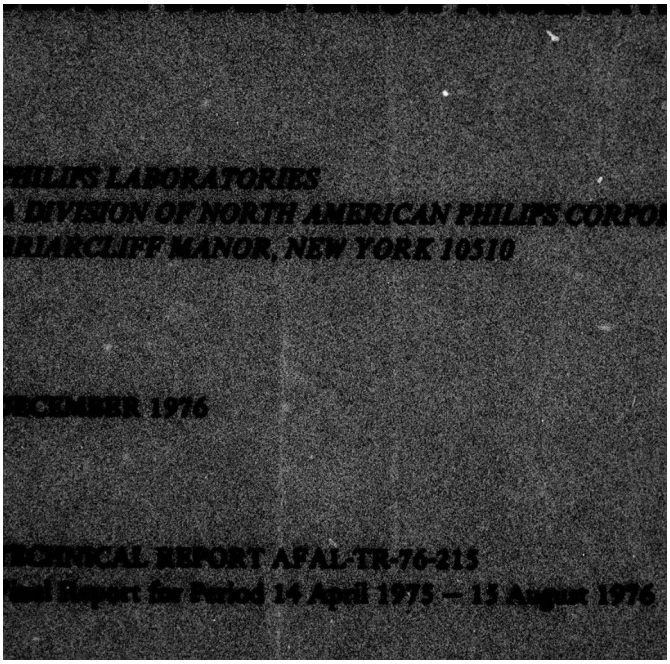
PHILIPS LABORATORIES
A DIVISION OF NORTH AMERICAN PHILIPS CORPOR
BRIARCLIFF MANOR, NEW YORK 10510
DECEMBER 1976
TECHNICAL REPORT AFAL-TR-76-215
Final Report for Period 14 April 1975 – 15 August 1976

UNCLASSIFIED

SECURITY CLASSIFICATION OF THIS PAGE (When Data Entered)

REPORT DOCUMENTATION PAGE

READ INSTRUCTIONS BEFORE COMPLETING FORM

1. REPORT NUMBER: AFAL-TR-76-215	2. GOVT ACCESSION NO.
3. RECIPIENT'S CATALOG NUMBER	
4. TITLE (and Subtitle): GROWTH OF HIGH-QUALITY CESIUM DIDEUTERIUM ARSENATE CRYSTALS	5. TYPE OF REPORT & PERIOD COVERED: Final Report, 14 Apr 75 - 15 Aug 76
6. PERFORMING ORG. REPORT NUMBER	
7. AUTHOR(s): G.M. Loiacono, W.N. Osborne, M. Delfino	8. CONTRACT OR GRANT NUMBER(s): Contract F33615-75-C-1202
9. PERFORMING ORGANIZATION NAME AND ADDRESS: Philips Laboratories, A Division of North American Philips Corporation, Briarcliff Manor, New York 10510	10. PROGRAM ELEMENT, PROJECT, TASK AREA & WORK UNIT NUMBERS: 2001-01-40, 01
11. CONTROLLING OFFICE NAME AND ADDRESS: Air Force Avionics Laboratory, Air Force Systems Command, Wright-Patterson Air Force Base, Ohio 45433	12. REPORT DATE: December 1976
	13. NUMBER OF PAGES: 64
14. MONITORING AGENCY NAME & ADDRESS (if different from Controlling Office): 62204F, 73 p.	15. SECURITY CLASS. (of this report): UNCLASSIFIED
	15a. DECLASSIFICATION/DOWNGRADING SCHEDULE

16. DISTRIBUTION STATEMENT (of this Report)

Approved for public release; distribution unlimited.

17. DISTRIBUTION STATEMENT (of the abstract entered in Block 20, if different from Report)

18. SUPPLEMENTARY NOTES

19. KEY WORDS (Continue on reverse side if necessary and identify by block number)

cesium dideuterium arsenate crystals

crystal growth conditions

20. ABSTRACT (Continue on reverse side if necessary and identify by block number)

The growth of cesium dideuterium arsenate (CsD_2AsO_4) crystals from aqueous and mixed solvent systems was studied, with emphasis on the problems of tapering and flawing. Fluid flow, seed orientation, deuteration, impurities, pH and saturation temperature had negligible effects on taper. An empirical process for growing taper-free CsD_2AsO_4 was developed. This process consists of initial capping of a seed plate in D_2O solvent followed by growth of the capped seed in a D_2O/glycol solvent. The optical absorption, 90° phase-matching temperature, and thermal stability of CsD_2AsO_4 as a function of deuteration were determined. A high-temperature

DD FORM 1 JAN 73 1473 EDITION OF 1 NOV 65 IS OBSOLETE

UNCLASSIFIED

SECURITY CLASSIFICATION OF THIS PAGE (When Data Entered)

degree

387 334

20. ABSTRACT (Continued)

(409°K), destructive, phase transition was discovered in CsD_2AsO_4. As a result, a compromise between optical absorption and the 90° phase-matching temperature must be made. Six crystals were characterized and delivered.

PREFACE

This is the Final Technical Report by Philips Laboratories, a Division of North American Philips Corporation, Briarcliff Manor, New York on the growth of cesium dideuterium arsenate crystals.

The program was sponsored by The Air Force Avionics Laboratory, Air Force Systems Command, Wright-Patterson Air Force Base, Ohio. Mr. Michael M. Heil (AFAL/DHO) was the Project Engineer.

The authors wish to thank the following personnel at Philips Laboratories who contributed to the theoretical and experimental phases of this program: S.K. Kurtz, F. Zernike, J. Ladell, J. Dougherty, W. Mueller-Herget, J. Nicolosi, M. Nelson, and S. Cangelosi.

TABLE OF CONTENTS

LIST OF ILLUSTRATIONS

LIST OF ILLUSTRATIONS (Cont'd)

LIST OF TABLES

SECTION I
INTRODUCTION

Cesium dideuterium arsenate, $Cs(D_xH_{1-x})_2AsO_4$, is a solid-solution compound of CsD_2AsO_4 and CsH_2AsO_4. The value of x depends on the initial deuteration level in the crystal growth solution and on the crystal growth parameters. Previous work has shown that the composition $Cs(D_{0.856}H_{0.144})_2AsO_4$ can be obtained from solutions containing an initial deuteration of 93 mole % (Refs. 1, 2). For purposes of this report, the compositional formula is given as CsD_2AsO_4 - which will be considered an approximation.

While CsD_2AsO_4 holds great promise for high-power, second harmonic generation (SHG), the optimization of crystal quality, properties, and size has not been achieved (Refs. 1-5). The major difficulty in the growth of single-crystal CsD_2AsO_4 has been the lack of data on the solution chemistry of the growth system.

In a final report of a previous program, the specific problems associated with the growth of CsD_2AsO_4 are detailed, and preliminary data indicated that a suitable solvent system appeared to be D_2O-glycol (Ref. 1). The problems encountered in the crystal growth of CsD_2AsO_4 from D_2O were: flawing, tapering, edge and corner growth, and irregular changes in solubility. All of these problems should be controllable by suitable adjustments of the supersaturation in the growing solution, and, to a large extent, they had been minimized by use of the mixed solvent D_2O-$(CH_2)_2(OD)_2$ at the 70/30 ratio. One problem that was not described in the above report was the availability of large quality, seed crystals. For example, an SHG crystal with a clear aperture of 1.5 x 1.5 cm and a length of 2.5 cm would require an initial seed plate with dimensions 3.5 x 3.5 cm. However, this plate is larger than material presently available or known to exist.

The goals of the present program were: to investigate variations in solution-growth parameters in order to determine a set of optimum conditions for the repeatable growth of large, highly deuterated, low-optical-loss CsD_2AsO_4 crystals; and to characterize and deliver sample crystals. This was accomplished by a systematic evaluation of the changes in solution chemistry of the compound and of the effects of growth parameters. During the program, data were obtained at various mixed-solvent ratios in order to determine feasibility of CsD_2AsO_4 growth, and the crystals were characterized with respect to optical absorption and deuteration levels.

SECTION II

PHYSICAL AND CHEMICAL PROPERTIES OF CsD_2AsO_4

2.1 Crystallographic Data

Cesium dideuterium arsenate (CsD_2AsO_4) belongs to the tetragonal system, space group $I\bar{4}2d$, and has a tetramolecular unit cell. Other crystals which are members of this class are KH_2PO_4, RbH_2AsO_4, $NH_4H_2PO_4$ and KH_2AsO_4. Table 1 lists the lattice

TABLE 1: Lattice parameters for $Cs(D_xH_{1-x})_2AsO_4$ (Powder Data).

	$Cs(D_{0.86}H_{0.14})_2AsO_4$	$Cs(D_{0.056}H_{0.144})_2AsO_4$
a_o	7.985 ± 0.004 Å	7.982 ± 0.005 Å
c_o	7.896 ± 0.004 Å	7.888 ± 0.005 Å
d_x	3.634 g/cm^3	3.641 g/cm^3
Space Group	$I\bar{4}2d$	$I\bar{4}2d$
Reference	present work	Ref. 1

parameters representative of CsD_2AsO_4 prepared during this study and compares them with previously published values. The data were obtained at 22°C.

It should be noted that the lattice parameters for CsH_2AsO_4 are nearly identical to those for the deuterated crystal: a_o = 7.98 Å and c_o = 7.87 Å with d_x = 3.62 g/cm^3 (Ref. 6). The indexed powder diffraction pattern for $Cs(D_{0.86}H_{0.14})_2AsO_4$ is illustrated in Figure 1. The source radiation was Ni filtered Cu at 40 kV and 30 mA. The eight strongest lines are listed in Table 2. The systematic absences are consistent with the space group $I\bar{4}2d$.

A computer print-out of all indexed lines is given in Appendix A. The values of the listed reciprocal lattice parameters represent the best values as determined up to the particular line. Thus, for example, for the line beginning with "512 1.4556_ _ _", A* = 0.19297 and C* = 0.19514 were determined from observational equations using the data from the preceding

Figure 1: Standard powder diffraction pattern for $Cs(D_{0.86}H_{0.14})_2AsO_4$.

TABLE 2: Powder X-ray lines for $Cs(D_{0.86}H_{0.14})_2AsO_4$.

Line #	d-spacing	Relative Intensity	Index
1	3.2329	100	112
2	2.1266	86	312
3	3.9923	61	200
4	1.4556	35	512
5	2.8215	31	220
6	1.7694	29	204
7	1.6990	25	332
8	1.3241	23	424

19 indexed lines. Lines with asterisks could not be indexed on the basis of the assumed cell, and imposed analytic constraints. The unindexed lines are weak lines, four of these are actually beta lines.

The structure and lattice parameters for single-crystal $Cs(D_{0.86}H_{0.14})_2AsO_4$ were also determined on the Buerger precession camera. Figure 2 is a set of full precession photos taken with Mo radiation at 50 kV, 35 mA at 22°C. The intensities and systematic absences of the diffraction spots show that the crystal belongs to the tetragonal system with space group $I\bar{4}2d$. The lattice parameters calculated from this data are $a_o = 7.984 \pm 0.005$ Å, $c_o = 7.899 \pm 0.005$ Å, and are in excellent agreement with the powder values.

Table 3 compares the lattice parameters of CsD_2AsO_4 with other members of the KH_2PO_4 family. In general, the lattice parameters slightly increase on deuteration with the exception of the Cs salt. Two points relevant to the crystal growth problem can be assumed. First, the negligible difference in lattice parameters between CsH_2AsO_4 and CsD_2AsO_4 would indicate the former could be used as seed material. Second, the only other crystal which may be utilized as a seed would be RbH_2AsO_4 (or RbD_2AsO_4). The differences in lattice parameters

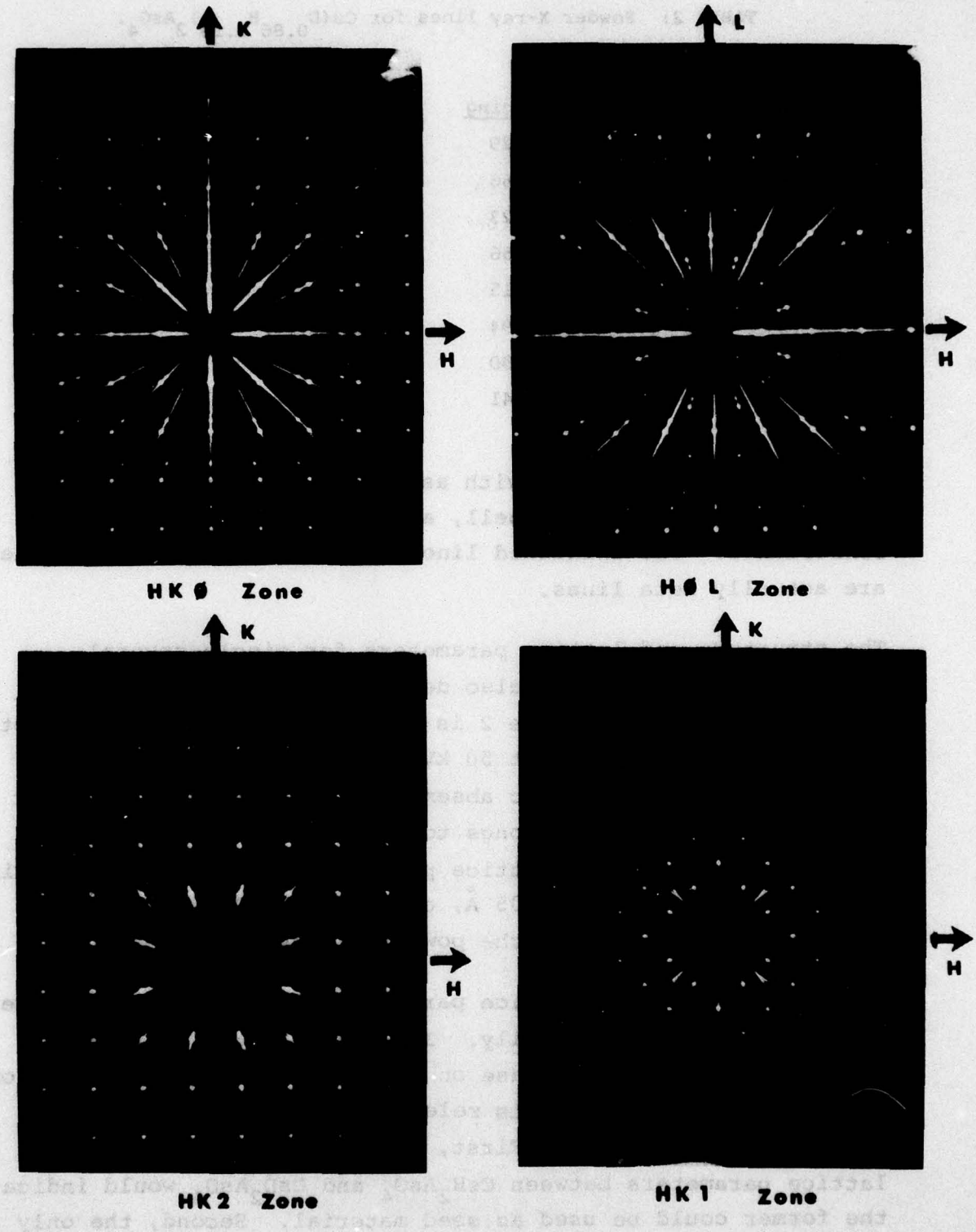

Figure 2: Precession photos taken with Mo radiation at 50 kV, 35 mA at 22°C.

TABLE 3: Lattice parameters of KH_2PO_4 family (Ref. 7).

Crystal	A_o (Å)	C_o (Å)	Temperature °C
KH_2PO_4	7.4529 ± .0002	6.9751 ± .0006	25°
KD_2PO_4*	7.4697 ± .0003	6.9766 ± .0005	25°
RbH_2PO_4	7.608 ± .008	7.296 ± .008	--
$NH_4H_2PO_4$	7.4991 ± .0004	7.5493 ± .0012	20°
$ND_4D_2PO_4$*	7.5193 ± .0009	7.5400 ± .0019	20°
KH_2AsO_4	7.6295 ± .0006	7.1605 ± .0008	25°
KD_2AsO_4*	7.6410 ± .0010	7.1636 ± .0009	25°
RbH_2AsO_4	7.7933 ± .0005	7.4671 ± .0005	25°
RbD_2AsO_4*	7.8063 ± .0007	7.4674 ± 0.0010	25°
CsH_2AsO_4	7.9852 ± .0004	7.8928 ± .0003	25°
$Cs(D_{0.86}H_{0.14})_2AsO_4$	7.985 ± .004	7.896 ± 0.004	22°
$NH_4H_2AsO_4$	7.6944 ± .0004	7.720 ± .002	25°

* deuteration levels unknown.

between the Rb and Cs salts are about 0.2 Å. It was found (see Par. 5.2) that CsH_2AsO_4 could be used as seed material for the growth of CsD_2AsO_4 but RbH_2AsO_4 resulted in dendritic growth. Therefore, the difference in lattice parameters (0.2 Å) exceeds some maximum value required for suitable crystal growth. Subsequently, it was determined that solid solutions of CsD_2AsO_4 and RbH_2AsO_4 do not exist over the entire composition range. According to the phase diagram this explains the formation of dendritic growth and the partial dissolution of RbH_2AsO_4.

2.2 Synthesis of CsD_2AsO_4

Table 4 lists the raw materials and impurity levels used for the synthesis of CsD_2AsO_4.

Two sources of arsenic were initially used to prepare deuterated arsenic acid. The use of $H_5As_3O_{10}$ was unsuitable due to the high impurity levels in the material available; subsequent work utilized As_2O_5. Aqueous solutions of both

As_2O_5 and Cs_2CO_3 were prepared by reacting stoichiometric quantities with D_2O. Great care was taken to use only slight excesses of D_2O above that required for stoichiometry.

TABLE 4: Raw material impurity levels (ppm)

Element	Cs_2CO_3	As_2O_5*	$H_5As_3O_{10}$*	D_2O
Li	<0.5	--	--	--
Na	2.9	--	--	2
K	2.6	--	--	--
Rb	45	--	--	--
Ca	<0.5	--	10	<0.5
Mg	<0.5	--	10	<0.3
Sr	<1.0	--	--	--
Ba	<10.0	--	--	--
Al	8	--	--	1
Fe	0.3	<1	10	0.5
Cr	<0.1	--	--	<0.1
Bi	--	--	10	--
B	--	--	--	<0.1
Ni	--	--	--	<0.5
Cu	--	--	10	--
Sb	--	<10	100	--
Mn	<1.0	--	--	0.1
Pb	--	<10	100	--
S	<5	--	--	--
P	<0.5	--	--	--
Si	1.3	--	100	5
Ti	--	--	100	<0.1

-- not detected

* Vendor supplied analysis:

Cs_2CO_3 : Supplied by Apache Chemical Co., Seward, Illinois

As_2O_5 : Supplied by Apache Chemical Co., Seward, Illinois

D_2O : Supplied by U.S. Atomic Energy Comm.

$H_5As_3O_{10}$: Supplied by Cerac/Pure Inc., Butler, Wis.

High-purity, nitrogen flushes were employed during preparation in order to minimize deuterium-hydrogen exchange with the atmosphere. The basic reaction for the synthesis of CsD_2AsO_4 is:

$$Cs_2CO_{3(aq.)} + 2D_3AsO_{4(aq.)} \rightleftarrows D_2O + 2CsD_2AsO_{4(aq.)} + CO_2\uparrow \quad (1)$$

The two reactants were slowly mixed at 60°C, and the resultant solution cooled to room temperature. Due to the extremely high solubility of CsD_2AsO_4 in D_2O, vacuum distillation was used to further precipitate CsD_2AsO_4 from solution. All crystalline CsD_2AsO_4 employed in saturation point adjustments was recrystallized twice.

All solutions used for crystal growth were filtered hot (15°C above saturation) through a 0.6 μm teflon millipore filtration system under a nitrogen atmosphere. The filtered solutions were loaded directly into the crystallizers immediately after filtration.

Compositional analysis for Cs and As in the starting materials indicated the need for drying Cs_2CO_3 and CsD_2AsO_4 before measurements were performed. For example, the theoretical weight fraction of Cs present in Cs_2CO_3 is 73.43%. A chemical analysis of the carbonate yielded a value of 80.23% prior to drying and a value of 73.10% after drying. In the case of CsD_2AsO_4, the values for Cs and As before and after drying were Cs: 48.6 and 48.4% (theory: 48.2%) and As: 25.9% and 27.2% (theory: 27.2%).

SECTION III

THE CsD_2AsO_4 - D_2O SYSTEMS

3.1 Phase Stability

CsD_2AsO_4 was found to be one stable crystalline phase in the ternary system Cs_2O-As_2O_5-D_2O at 25°C over the pH range 3 to 9 (Ref. 1). To further study the solution properties of the CsD_2AsO_4-D_2O system, a titration curve of D_3AsO_4 with Cs_2CO_3 was prepared. The pH range over which CsD_2AsO_4 exists in solution was determined. Figure 3 illustrates the data. The range of pH over which CsD_2AsO_4 can be formed extends from pH 3 to 8.5 at 22°C. Adjustment of growth solutions to pH values outside this range will result in second phase precipitation. Below pH 3, one can expect a mixture of CsD_2AsO_4 and D_3AsO_4, and above pH 8.5, CsD_2AsO_4 and Cs_2DAsO_4 mixtures. The stoichiometric pH for the system occurs at pH 4.85.

3.2 Solubility

The solubility curve of CsD_2AsO_4 in D_2O was examined and found to be in agreement with that previously reported (Ref. 1). Only three points were checked; agreement with within 10%.

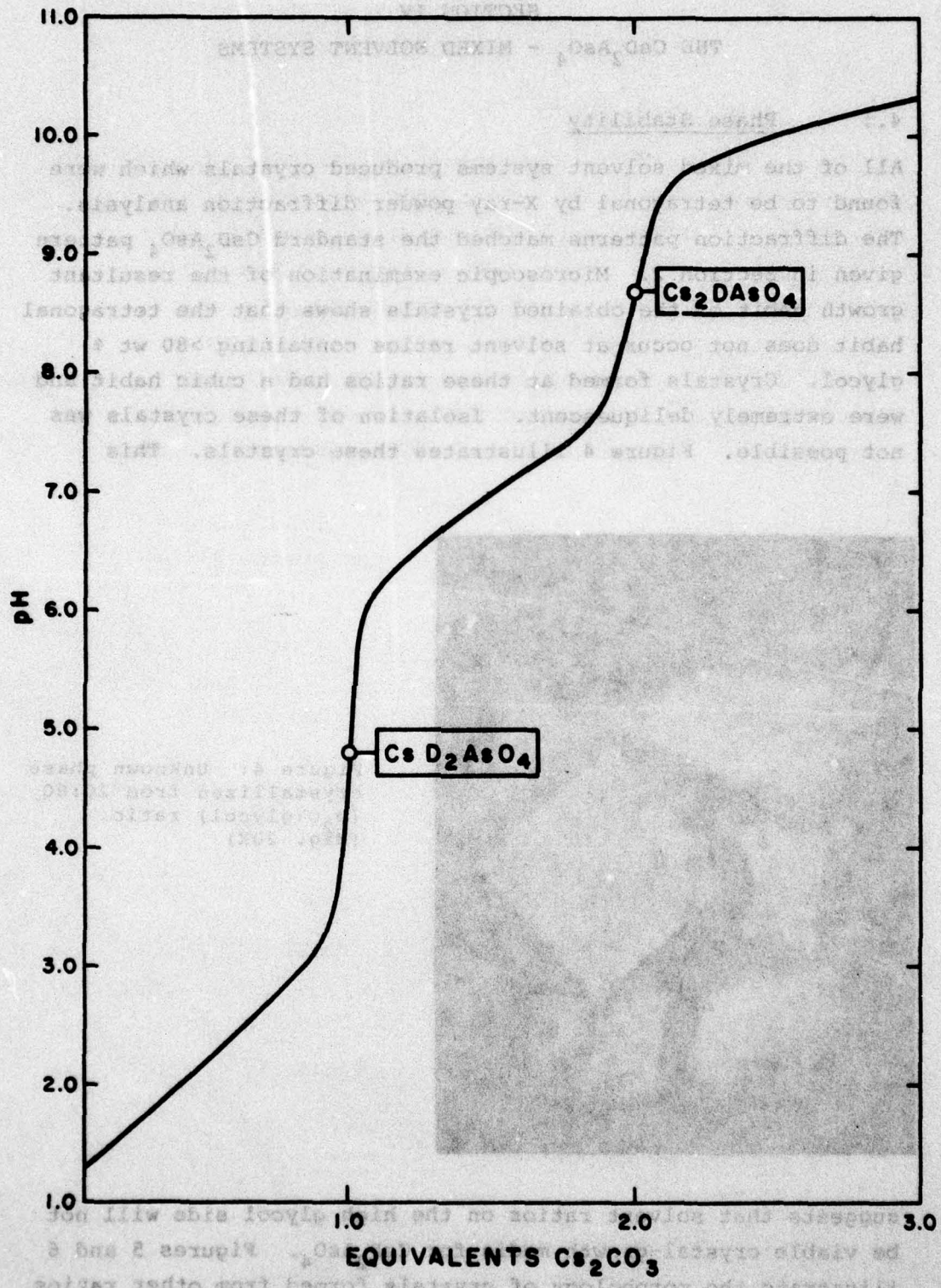

Figure 3: Titration curve of $D_3AsO_{4(aq.)}$ with $Cs_2CO_{3(aq.)}$.

SECTION IV

THE CsD_2AsO_4 - MIXED SOLVENT SYSTEMS

4.1 Phase Stability

All of the mixed solvent systems produced crystals which were found to be tetragonal by X-ray powder diffraction analysis. The diffraction patterns matched the standard CsD_2AsO_4 pattern given in Section 2. Microscopic examination of the resultant growth habit of the obtained crystals shows that the tetragonal habit does not occur at solvent ratios containing >80 wt % glycol. Crystals formed at these ratios had a cubic habit and were extremely deliquescent. Isolation of these crystals was not possible. Figure 4 illustrates these crystals. This

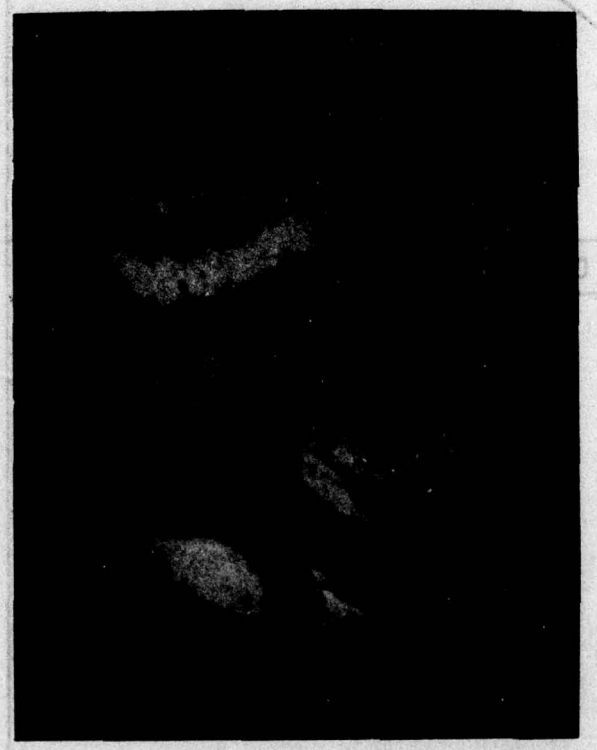

Figure 4: Unknown phase crystallized from 20:80 (D_2O:glycol) ratio. (Mag. 20X)

suggests that solvent ratios on the high glycol side will not be viable crystal-growth media for CsD_2AsO_4. Figures 5 and 6 illustrate the morphology of crystals formed from other ratios

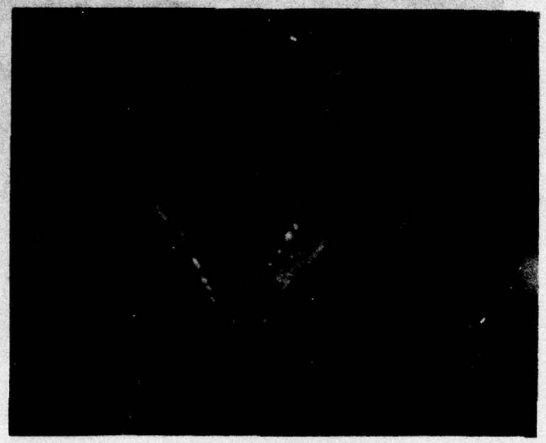

(a) 100 D_2O

(b) 70 Glycol-30 D_2O

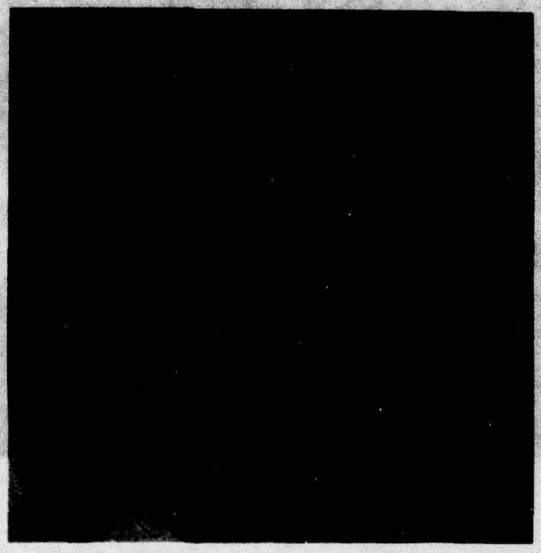

(c) 30 Glycol-70 D_2O

Figure 5: Morphology of CsD_2AsO_4.

(a) 50 Glycol-50 D_2O

(b) 20 MeOH-80 D_2O

(c) 30 MeOH-70 D_2O

Figure 6: Morphology of CsD_2AsO_4.

of D_2O-CH_3OH and D_2O-glycol. These crystals were formed under static growth conditions on the bottom of the containing vessels. The solutions were saturated at 50°C with crystalline CsD_2AsO_4 and the pH adjusted to 5.0. The rate of temperature decrease was 1°/day over a two week period. The photographs are magnified approximately seven times. It is apparent that the normal tetragonal habit, taper-free, is only obtained from pure D_2O (Fig. 5a). The {101} faces are perfectly formed and {100} prism faces show no evidence of tapering. This would suggest that crystal growth under static conditions (zero rotation) should result in taper free boules. Full scale growth experiments did not support this speculation. The crystal morphology in both the glycol-D_2O and methanol-D_2O systems exhibited severe tapering and abnormal {101} pyramid faces.

4.2 Solubility

The solubilities of CsD_2AsO_4 in methanol, ethanol, and glycol [CH_3OH; C_2H_5OH; $(CH_2)_2(OH)_2$] and various mixtures with D_2O were determined. Initially, H_2O was used and the data is directly related to the D_2O case except that the solubility of CsD_2AsO_4 is about 25% higher. Ethanol and H_2O are completely miscible, (except that when CsD_2AsO_4 is added it caused two liquid phases to separate at room temperature (22°C) saturation). This mixed solvent system is not viable in the volume ratios 50:50, 80:20 and 20:80 (H_2O/C_2H_5OH). Increasing the temperature of these ratios had no effect on the system -- two liquid phases were still observed. The two-phase behavior of the CsD_2AsO_4-C_2H_5OH-H_2O system was not expected and this behavior is unexplained.

The substitution of methanol (CH_3OH) for ethanol as a component in a mixed solvent system was examined at six ratios. The ratios (D_2O/CH_3OD) of 50:50 and 40:60 did not separate into two liquid phases upon addition of CsD_2AsO_4, but spontaneous nucleation occurred on the container walls during cooling such that controlled crystal growth is unlikely. Crystallization of material from this solvent system indicated that this mixture was an

unsuitable solvent. Table 5 lists the solubility of CsD_2AsO_4 in the D_2O/CH_3OH solvent at 22°C for various ratios. Comparison of this data with that of the $D_2O/(CH_2)_2(OH)_2$ system previously

TABLE 5: System CsD_2AsO_4 - D_2O-CH_3OH @ 22°C

Solvent Ratio D_2O/CH_3OH		Solubility of CsD_2AsO_4
Volume %	Weight %	g/100 g
90:10	92:8	132
80:20	83:17	110
70:30	75:25	106
60:40	66:34	77

reported indicates the higher D_2O/CH_3OH ratios may be a viable growing medium for CsD_2AsO_4 (Ref. 1). A plot of the solubility of CsD_2AsO_4 as a function of solvent ratio (at 22°C) is shown in Figure 7, for both the D_2O/CH_3OH and $H_2O/(CH_2)_2(OH)_2$ mixed solvents. The data points for the methanol system show that at any specific ratio, the solubility of CsD_2AsO_4 is reduced considerably. Suitable growth media could possibly exist in this system.

The solubility of CsD_2AsO_4 in the $D_2O/(CH_2)_2(OD)_2$ mixed solvent system is shown in Table 6. This data was obtained over the temperature range 26°C to 57°C at pH 4.8. Considerable

TABLE 6: Solubility data for CsD_2AsO_4 in various D_2O:$(CH_2)_2(OD)_2$ solvent ratios (g/100 g solvent).

Solvent Composition $(D_2O:C_2H_4(OD)_2$	Temperature (°C)						
	57°	52°	46°	42°	36°	31°	26°
100:0	-	310	268	283	260	270	252
70:30A*	277	309	266	271	282	249	245
70:30B	274	298	266	248	281	252	249
50:50A	202	230	183	203	-	187	182
50:50B	212	224	211	200	-	149	181
30:70A	242	265	246	236	-	222	215
30:70B	244	264	245	235	222	220	215

*A, B denote duplicate samples measured.

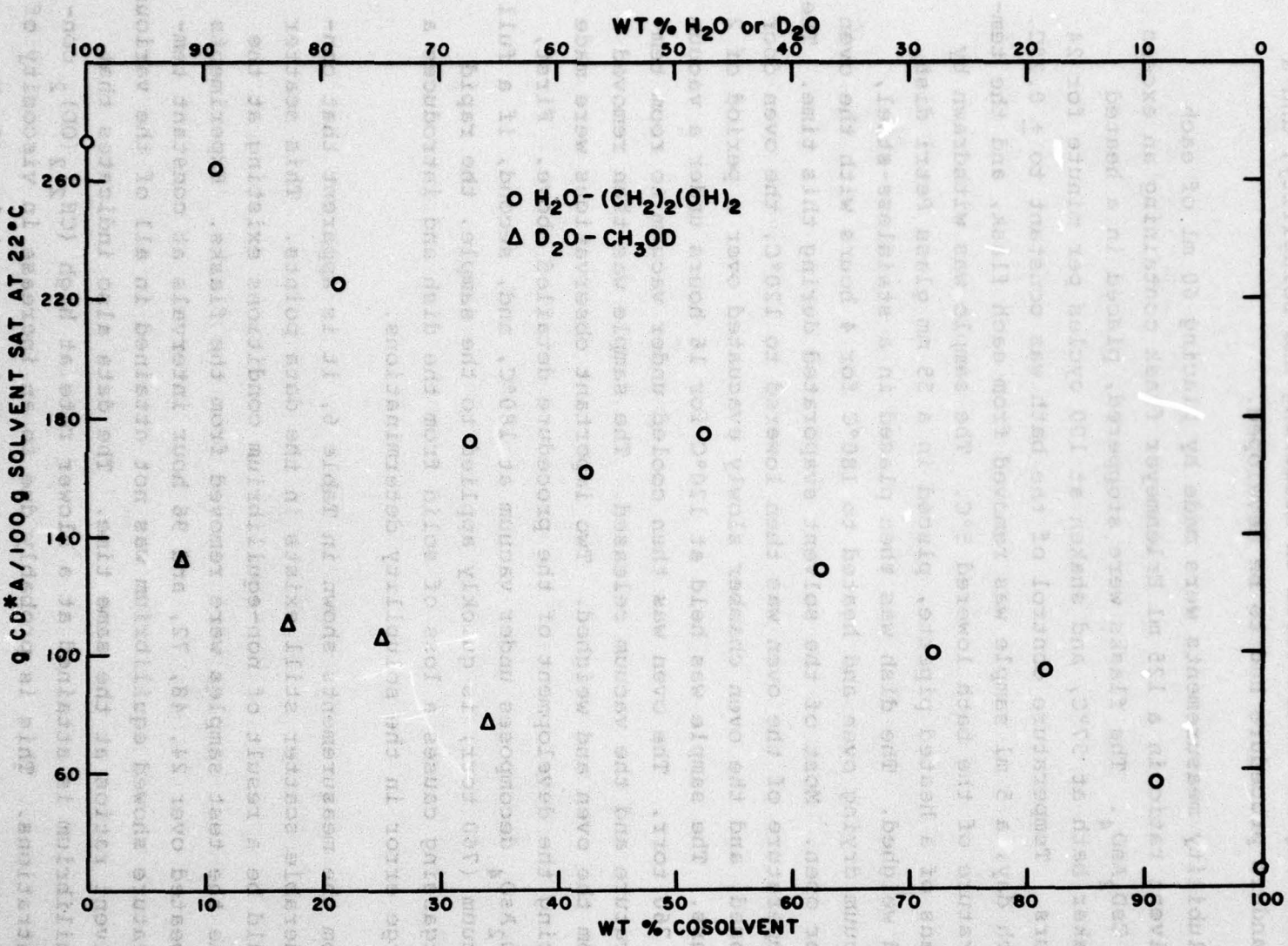

Figure 7: Solubility of CsD_2AsO_4.

difficulty was encountered in measuring the solubility, and a standard procedure had to be developed.

Solubility measurements were made by placing 60 ml of each solvent ratio in a 125 ml Erlenmeyer flask containing an excess of CsD_2AsO_4. The flasks were stoppered, placed in a heated shaker bath at 57°C, and shaken at 100 cycles per minute for 24 hours. Temperature control of the bath was constant to $\pm$ 0.2°C. Each day, a 5 ml sample was removed from each flask, and the temperature of the bath lowered 5°C. The sample was withdrawn by means of a heated pipette, placed in a 55 mm glass Petri dish, and weighed. The dish was then placed in a stainless-steel, vacuum drying oven and heated to 180°C for 4 hours with the oven door open. Most of the solvent evaporated during this time. The temperature of the oven was then lowered to 120°C, the oven door closed, and the oven chamber slowly evacuated over a period of 2 hours. The sample was held at 120°C for 16 hours under a vacuum of 760 torr. The oven was then cooled under vacuum to room temperature and the vacuum released. The sample was then removed from the oven and weighed. Two important observations were made during the development of the procedure detailed above. First, CsD_2AsO_4 decomposes under vacuum at 180°C, and, second, if a full vacuum (760 torr) is quickly applied to the sample, the rapid outgassing causes a loss of solid from the dish and introduces a large error in the solubility determinations.

From the measurements shown in Table 6, it is apparent that considerable scatter still exists in the data points. This scatter could be a result of non-equilibrium conditions existing at the time the test samples were removed from the flasks. Experiments repeated over 24, 48, 72, and 96 hour intervals at constant temperature showed equilibrium was not attained in all of the various solvent ratios at the same time. The data also indicates that equilibrium is attained at a slower rate at high $(CH_2)_2(OD)_2$ concentrations. This is probably due to an increase in viscosity of the solvent system. Measurements on duplicate samples (A, B, Table 6) show a reproducibility of >95%. It is evident that the

aquisition of a meaningful set of solubility data requires that the data be obtained over an extended period of time.

The solubility data obtained resulted in a surprising observation. Figure 8 illustrates the data obtained in terms of solute-to-solvent mole ratio and solvent composition. From this figure it can be seen that the number of moles of solvent per mole of CsD_2AsO_4 as a function of solvent ratio remains a constant (~5.5) up to about 15 weight % D_2O. At this point, the curve increases rapidly. This is also the point where tetragonal CsD_2AsO_4 fails to crystallize and cubic crystals of unknown composition are obtained. It is evident that the use of D_2O-$(CH_2)_2(OD)_2$ as a mixed solvent system for the purpose of decreasing the degree of association in the crystallizing solution is not feasible. Part of the rationale of using a mixed solvent system to reduce the solubility of CsD_2AsO_4 was to effectively decrease the degree of association in the crystallizing solution. This would result in an increase in the number of solvent molecules and in the completion of the primary hydration (solution) sphere around the CsD_2AsO_4 molecules.

An initial survey of possible new solvents for CsD_2AsO_4 based on solvent dielectric properties was completed. The results are summarized in Table 7. In all cases where a measurable solubility was observed, the appearance of multiple crystalline phases was detected. The possibility of identifying a pure suitable substitute solvent for CsD_2AsO_4, where only the required tetragonal phase crystallizes, appears to be remote.

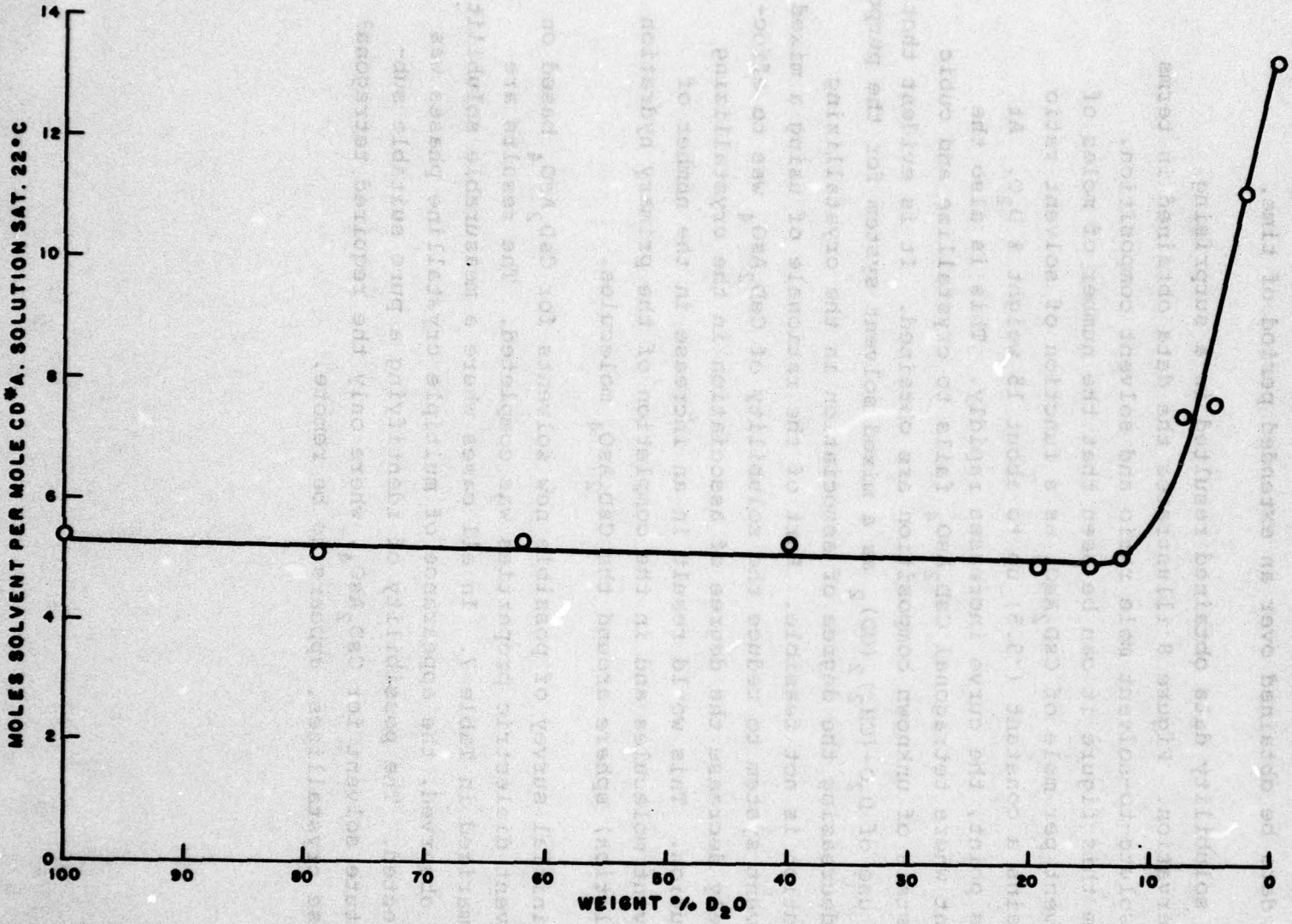

Figure 8: Solute-to-solvent mole ratio vs. solvent ratio in CD*A - ethylene glycol - D_2O system.

TABLE 7: Summary of solvent survey (25°C)

Solvent	Dielectric Constant at 25°C	Observations *
Methanol	33	M, SS
Ethanol	24	M, I
2-Propanol	18	M, I
1, 4 Dioxane	2	I
Ethylene Glycol	--	M, 33.5g/100g
Acetonitrile	36	M, > 10g/100g
Formamide	109	M, > 10g/100g
Pyridine	12	I
Carbon Tetrachloride	2	I
Carbon Disulfide	--	M, I
Diethyl Ether	4	I
Tetrahydrofuran	7	M, > 10g/100g
Benzene	2	I
Toluene	2	I
O-Xylene	--	I

* I = insoluble < 2g/100g solvent
SS = slightly soluble < 10g/100g solvent
M = mixed phases

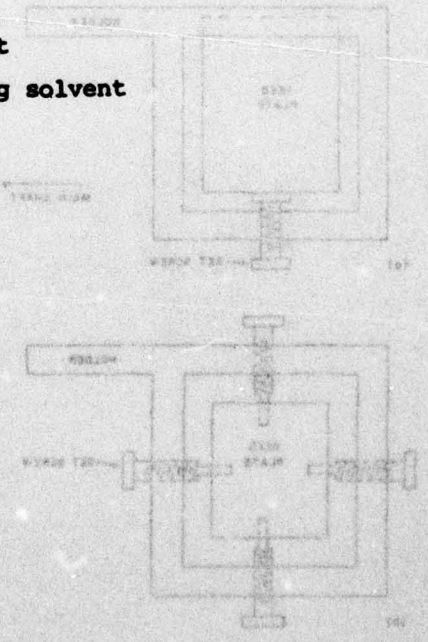

SECTION V
CRYSTAL GROWTH EXPERIMENTS

5.1 Preparation of Seed Materials

Large area seed plates $(2.5\ cm)^2$ of CsD_2AsO_4 are unavailable. The largest crystals known were produced under a previous Government program (Ref. 1). Some of these crystals were furnished by Dr. Fred Quelle, of the Office of Naval Research, Boston, through Mr. Michael Heil of the Air Force Avionics Laboratory. Unfortunately only small flawless seed plates $(1.5\ cm)^2$ could be salvaged from these highly flawed crystals. Larger seed plates $(\sim 2.5\ cm)^2$ containing twins and numerous flaws were also fabricated from the remaining material.

In all the crystal growth runs, only Z-plates or capped boules were used except for one run made with a boule whose caps had been fabricated into 45° faces. The plates or caps were mounted in either of the two seed holders shown in Figure 9. The differences in growth behavior will be discussed in the following sections. Usually only one crystal was mounted in the crystallizer during a run.

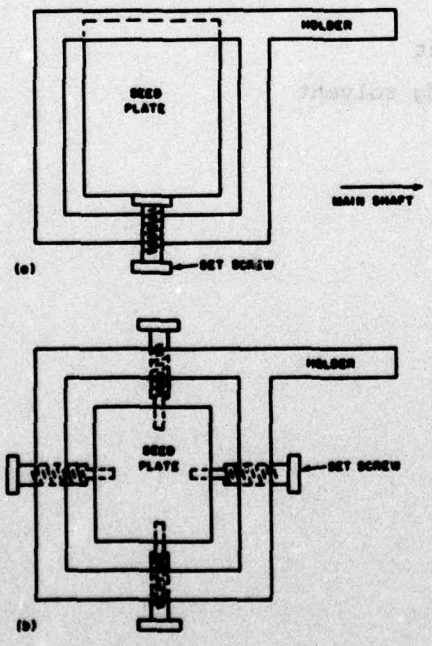

Figure 9: Seed holding methods.

Another possible source of seed material for CsD_2AsO_4 growth is to use a crystal of similar structure. Based on the X-ray data available for the lattice parameters of other members of the tetragonal KH_2PO_4 family, only two materials had a minimum lattice mismatch with CsD_2AsO_4. These were RbH_2AsO_4 and CsH_2AsO_4. In fact, the lattice mismatch between CsH_2AsO_4 and CsD_2AsO_4 is less than one part in a hundred. The largest commercially available Z-plates (20 x 20 mm) of both materials were purchased.

An important consideration in the growth of CsD_2AsO_4 is the method used to hold the seed crystal. It is evident from data previously taken, that mounting of the seed plate with the Z-axis in a parallel position to the axis of rotation is undesirable (Ref. 1). All seed plates were mounted so that the {101} type faces were perpendicular to the liquid flow caused by the rotation of the seed holder. In this case, the Z-axis is at right angles to the axis of rotation and results in a more uniform transport of growth media to the growing crystallographic faces. A consequence of this condition is a uniform growth rate.

There are two methods of seed attachment used in the preferred technique. The first is to drill four holes in the seed plate and subsequently fasten the plate to the seed holder using Teflon pins (Fig. 9b). These holes are prepared by use of a water drill and cause no strain to the seed. D_2O is used in place of water. The second method is to secure the seed plate by use of a thumb screw, with the top of the seed plate inserted into a bevel at the top of the holder (Fig. 9a). Both methods are schematically illustrated in Figure 9.

The latter method is routinely used in the growth of many solution grown crystals, such as KDP. It has one disadvantage in that the pressure required to hold the seed plate in place has a tendency to initiate X-Y growth at the points of contact of seed and holder. This always results in strained areas in

the crystals. The crystals also tend to grow over these points of contact, causing considerable difficulty in removal of the grown boule from the holder. The method of inserting four pins to support the seed plate is a modification of Holden's original spider configuration (Ref. 8). It has the distinct advantages of resulting in minimum strain to the seed plate during growth, and ease of boule removal, after growth. The only disadvantage of the method is that a considerable level of skill on the crystal grower's part is required to achieve equilibrium as quickly as possible in order to prevent excessive dissolution around the pins, thus causing the seed plate to fall out. This method was used in the present program for the bulk of the growth runs. The former method was used only when seed plates of sufficient thickness were not available.

The surface of the seed plates used for growth were D_2O-polished on felt. When seed caps were employed, no mechanical work was performed on the capped surface. As previously reported, (Ref. 1), no multiple twin growth resulted when perfect seed caps were used but almost all seed plates exhibited irregular growth and in many cases, the pyramid cap never formed. This can be attributed to the poor initial seed plate quality (i.e., voids, veils, etc.). It is obvious that a major problem in the growth of CsD_2AsO_4 is the lack of high quality seed material.

5.2 Crystal Growth

The following growth data were tabulated for each crystal growth run:

- Run No. and solution prep. ref.
- pH (initial and final)
- Solution volume
- Saturation temperature
- Rotation rate
- Seed dimensions (before and after)
- ΔT
- Total weight deposited
- g/°C
- g/liter solution
- Photograph of crystal

- Seed plate orientation
- Rate of temperature lowering
- Solution and crystal deuteration

Table 8 contains a compilation of selected parameters for the runs made during the program. The run number gives the actual chronological order in which the runs were performed. The pH of the solutions were read at 20°C using reference buffers for calibration of the meter. The accuracy of the recorded pH was ± 0.002 units. The saturation temperatures of each run were determined by suspending a seed of CsD_2AsO_4 in the solution and viewing the concentration currents emanating from the seed through an optical system. The precision of this method is ± 0.1°C. Seed dimensions were measured with a vernier (± 0.005 mm). A number of specific crystal growth runs have been selected to illustrate the difficulties involved in the growth of CsD_2AsO_4 crystals and are discussed below.

5.2.1 The Capping Process

One of the characteristics of CsD_2AsO_4 growth, common to all the KH_2PO_4 type crystals, is the process known as capping. The basic process consists of the development of {101} faces on a 0°Z plate. Figure 10 illustrates schematically the typical morphology of tetragonal CsD_2AsO_4 crystals and the

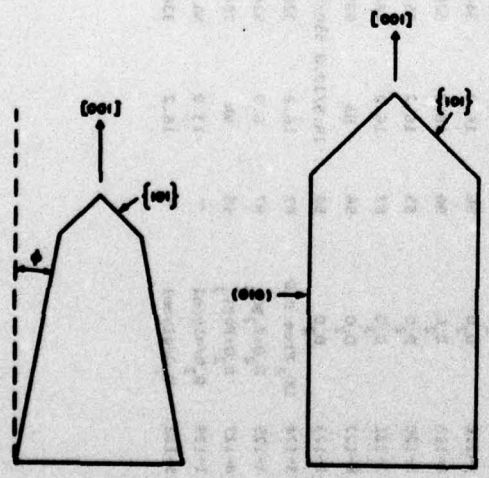

Figure 10: Morphology of tetragonal CsD_2AsO_4 crystals and taper angle (ϕ) for crystals of tetragonal symmetry.

TABLE 8: CsD_2AsO_4 crystal growth data.

Run #	Solvent Composition	Solvent %D	Rotation Velocity cm/s	Initial Seed Area mm^2	Solution pH @ 20°C	Saturation Temp °C	Solution Volume Liters	Δ T °C	Crystal Yield g/l/°C	Taper Angle Degrees	Comments
1-101	D_2O/glycol	74	7.2	576	5.6	52.5	4.3	1.2	--	11	Clear growth, controller failed - dissolved
1-102	70:30	68	7.2	702	7.2	44.8	4.2	3.9	5.3	0	Highly flawed, not capped
2-103	70:30	49	4.5	456	6.6	58.8	1.7	1.8	25.3	5	Cyclic flawing
8-104	70:30	60	--	360	6.5	47.9	2.0	0.8	55.6	6	Highly flawed
1-105	70:30	74	7.2	--	5.7	45.7	4.0	0.3	--	--	Edge growth, flawed, veils, spurious (45°Z)
3-107	70:30	67	3.2/6.5	576	7.1	20.5	2.1	5.9	--	15	Dissolved, controller failed, clear growth
1-108	D_2O (CDA Seed)	67	11.4/2.9	390	7.3	44.0	3.8	2.6	5.6	6	Clear growth
2-109	D_2O (RDA Seed)	74	--	675	7.3	40.0	2.0	--	--	--	Dendritic growth after 5° ΔT
2-113	D_2O	83	1.2/2.3	552	3.7	37.3	2.1	--	--	--	Variable dendritic growth
8-114	D_2O	96	16.2	--	8.1	47.0	2.0	--	--	--	Dissolved, controller failed
8-115	D_2O	96	16.2	288	8.1	49.5	1.9	0.6	37.7	5	Did not complete capping
8-116	D_2O	96	16.2	340	8.6	35.1	1.8	--	--	--	Dissolved
8-118	D_2O	96	16.2	528	7.2	30.4	1.7	--	--	--	Dissolved
8-120	D_2O	85	16.2	350	7.8	40.5	2.0	2.5	8.6	10	Clear growth
3-121	D_2O	87	16.2	480	7.2	17.5	2.1	6.1	3.2	7	Clear growth, twinned
8-122	D_2O	56	NA	895	7.6	44.8	2.0	6.5	10.1	13	Highly flawed, twinned
1-123	D_2O	56	19.5/13.8	550/386	7.6	44.8	6.0	3.0	6.7/2.7	14/10	Highly flawed
3-124	CO_2 Free D_2O	87	16.2	320	7.6	17.3	2.0	4.1	4.1	9	Clear growth, twinned
1-125	D_2O:H_2BO_3	87	6.9	520	7.4	35.6	2.0	2.6	--	13	Clear growth
8-127	D_2O:$FeCl_3$	56	NA	754	7.5	42.6	2.0	3.1	8.2	13	Flawed, some clear growth
1-129	D_2O/glycol	-	13.8	NA	7.5	46.5	2.1	2.0	--	6	Clear growth
5-133	D_2O/glycol	-	16.2	336	7.2	47.0	2.0	5.4	5.1	0	Clear growth

phenomenon of tapering - which is a serious problem in CsD_2AsO_4 crystal growth. The capping process is shown in Figure 11 and 12. In Figure 11 (a) a flat 0°Z plate mounted in the seed holder has begun to grow. On a macroscopic scale, one can observe that growth is rapid in the Z direction, with small individual pyramids forming, which ideally, will subsequently cohere to form the main growth pyramid. The mechanism involved in the capping process has not been explained but, empirically, can be related to formation of natural growth facets of low index and low surface energy (Ref. 10). This natural growth habit normally results in high quality crystal growth, except in the case of CsD_2AsO_4, an additional set of facets {301} develop which result in the taper angle. In subsequent steps (b) and (c), the macroscopic pyramids slowly form a completed cap. From these photographs, the crystal appears to be highly twinned, but after complete capping (e, f) clear single crystal growth is observed. The figures also indicate that tapering is initiated immediately at the start of growth (b) and that no X-Y growth, needed for development of seed cross section, is observed. The latter point was true for all growth runs made during this program.

The effect of the seed holder on the capping process is also illustrated in Figures 11 and 12. Both crystals were grown from the same solution under the identical conditions (Run #1-123) except for the method of seed holding. Figure 11 shows a flat 0°Z plate mounted with a thumb screw (see also Fig. 9a, 9b) while Figure 12 represents the pin arrangement. While both crystals tapered (14° and 10°), the amount of flawing in the thumb screw crystal is significantly greater. The recommended method for growth of CsD_2AsO_4 is the pin arrangement.

The effect of seed quality and orientation on the capping process was briefly examined. Unfortunately the lack of high quality seed material renders all observations inconclusive. It can be assumed that if high quality seed crystals were available, the capping process would not be characterized by a large number of individual crystallites growing into a twinned boule.

(a)

(b)

(c)

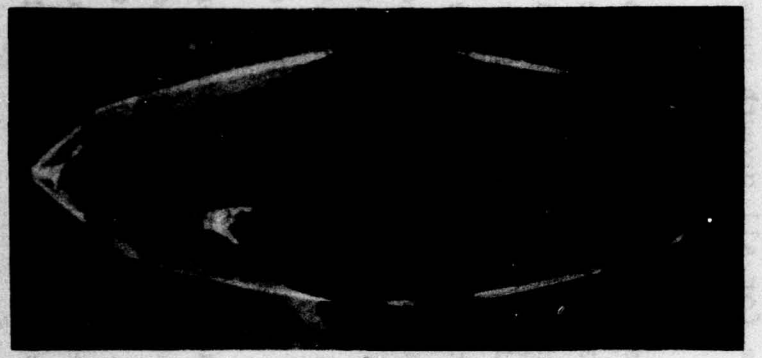

(d)

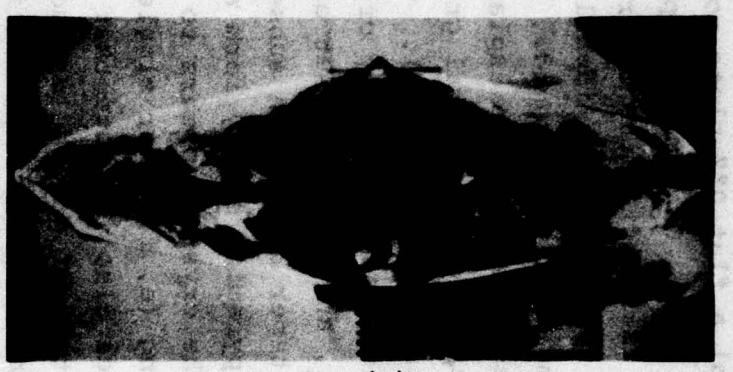

(e)

(f)

Figure 11: Effect of pressure-type seed holder on capping process (Run # 1-123).

(a)

(b)

(c)

(d)

(e)

(f)

Figure 12: Effect of pin-type seed holder on capping process (Run # 1-123).

5.2.2 pH Boundaries

Based on the titration curve previously discussed, both extremes of basic and acidic growth media were examined. Run #2-113 was made at pH 3.7. Figure 13 shows the CsD_2AsO_4 seed plate together

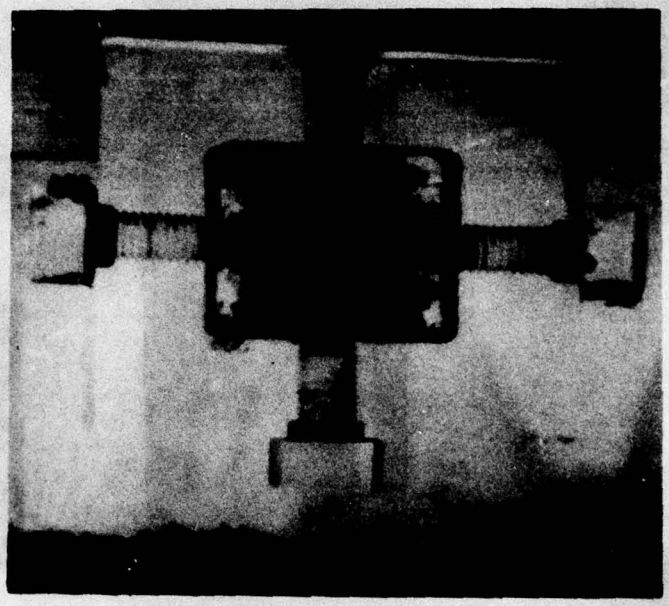

Figure 13: CsD_2AsO_4 growth at pH 3.7 (Run #2-113).

with dendritic growth and a considerable amount of spurious nucleation on the bottom of the crystallizer. X-ray diffraction analysis confirmed the dendritic growth to be non-tetragonal. Identification of the new phase was not attempted. A number of attempts to grow from solutions of pH 9.5 and 8.6 (Run #8-116) were unsuccessful. No growth could be initiated. These solutions are characterized by a continuous variation in pH on the order of $\pm$ 0.8 units. When the pH was lowered to 8.1 (Run #8-115) growth was observed, but the crystal did not cap. All growth runs were performed in the temperature range 35°-40°C.

Figure 14 illustrates a series of SEM photographs of the seed plate for Run #2-113. In (a), the plate has an amorphous appearance (30X). When higher magnifications were used (b, c) isolated single crystal sections imbeded in the amorphous matrix

(a) 30X (b) 600X (c) 1200X

Figure 14: SEM photograph of CsD_2AsO_4 seed plate (Run #2-113).

could be detected. The applicability of the titration curve to the CsD_2AsO_4 crystal growth system was confirmed.

5.2.3 Epitaxial Growth of CsD_2AsO_4 on CsH_2AsO_4 and RbH_2AsO_4 Seed Plates.

According to the lattice parameter mismatch, the best choices for epitaxial growth of CsD_2AsO_4 were CsH_2AsO_4 and RbH_2AsO_4. A growth solution of CsD_2AsO_4 was adjusted to pH 7.0 and the saturation point to 40°C. The RbH_2AsO_4 seed (2 x 2 cm) was rotated at 10 rpm with the solution flow parallel to the Z direction of the seed. The temperature of the growth solution was lowered 0.05°/day. After five days, the seed was still not growing. On the sixth day, the seed fell from the holder due to dissolution of material around the retaining pins. The growth run was continued, and the rate of temperature lowering increased to 0.1°/day. Within 24 hours, dendritic growth was observed on the seed surface. As growth continued, it became apparent that CsD_2AsO_4 can not be grown epitaxially on RbH_2AsO_4. The entire surface of the seed plate was covered with dendritic growth. These dendrites grew at an extremely high growth rate. This experiment was terminated. Figure 15 illustrates the

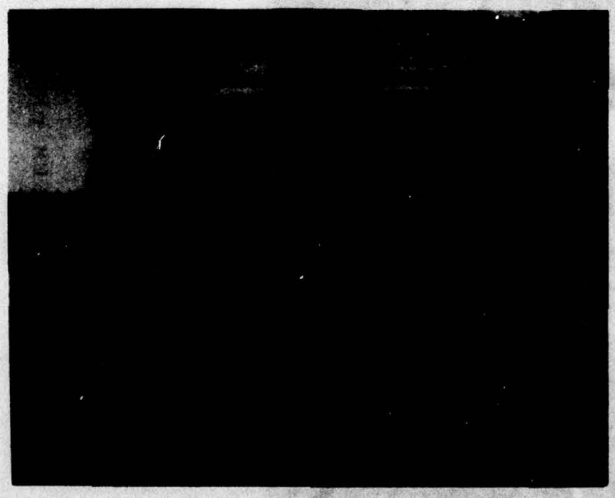

Figure 15: CsD_2AsO_4 growth on RbH_2AsO_4 seed (Run # 2-109).

RbH_2AsO_4 seed plate in situ prior to the plate dropping from the seed holder. The plate was apparently etched by the growth solution.

A second crystallizer (Run #1-108) was loaded with a CsH_2AsO_4 seed plate (Z axis; 2.0 x 2.0 cm). A solution of CsD_2AsO_4 saturated at 44°C and adjusted to pH 7.3 was used for growth. The solution temperature was lowered 0.03°/day. Based on observations described below for the low-temperature CsD_2AsO_4 growth run (see Par. 5.2.4), two rotation rates were used, i.e., 8 rpm counterclockwise and 32 rpm clockwise, with the same seed. Figure 16 is a series of photographs taken during this experiment for illustration of the taper and capping processes. The amount of Z growth required for capping at 8 rpm and 32 rpm was 18 mm and 14 mm, respectively. In terms of growth time, the side that rotated at 32 rpm capped four days sooner than that of the 8 rpm surface. An important effect was observed and is illustrated in Figure 16d. In the clear section of the cap growing in the 32 rpm direction, three parallel lines (flaws) can be observed. These flaws are parallel to (101) pyramid faces. They were generated during rotation in the opposite direction at 8 rpm. A 24 hour cycle was used for switching rotation directions and rotation rates. The spacing between these flaws corresponds to about 48 hours of growth. Therefore, the flaws were initially formed during rotation (at 8 rpm) in the opposite direction, and the clear or flawless region was generated when the rotation direction and rate were switched. This means that this growing surface had experienced "starvation" during the time period when rotation was at 8 rpm. Note also that the 8 rpm growing surface does not show the flaw effect when rotation was at 32 rpm, even through this region is a trailing edge. It is obvious that the high rotation rate increases the amount of material transport to the growing surface and that this may be the key to the growth of large, high optical-quality CsD_2AsO_4. The taper angle for this crystal is about 8° and does not appear to be affected by the rotation rates used in this experiment.

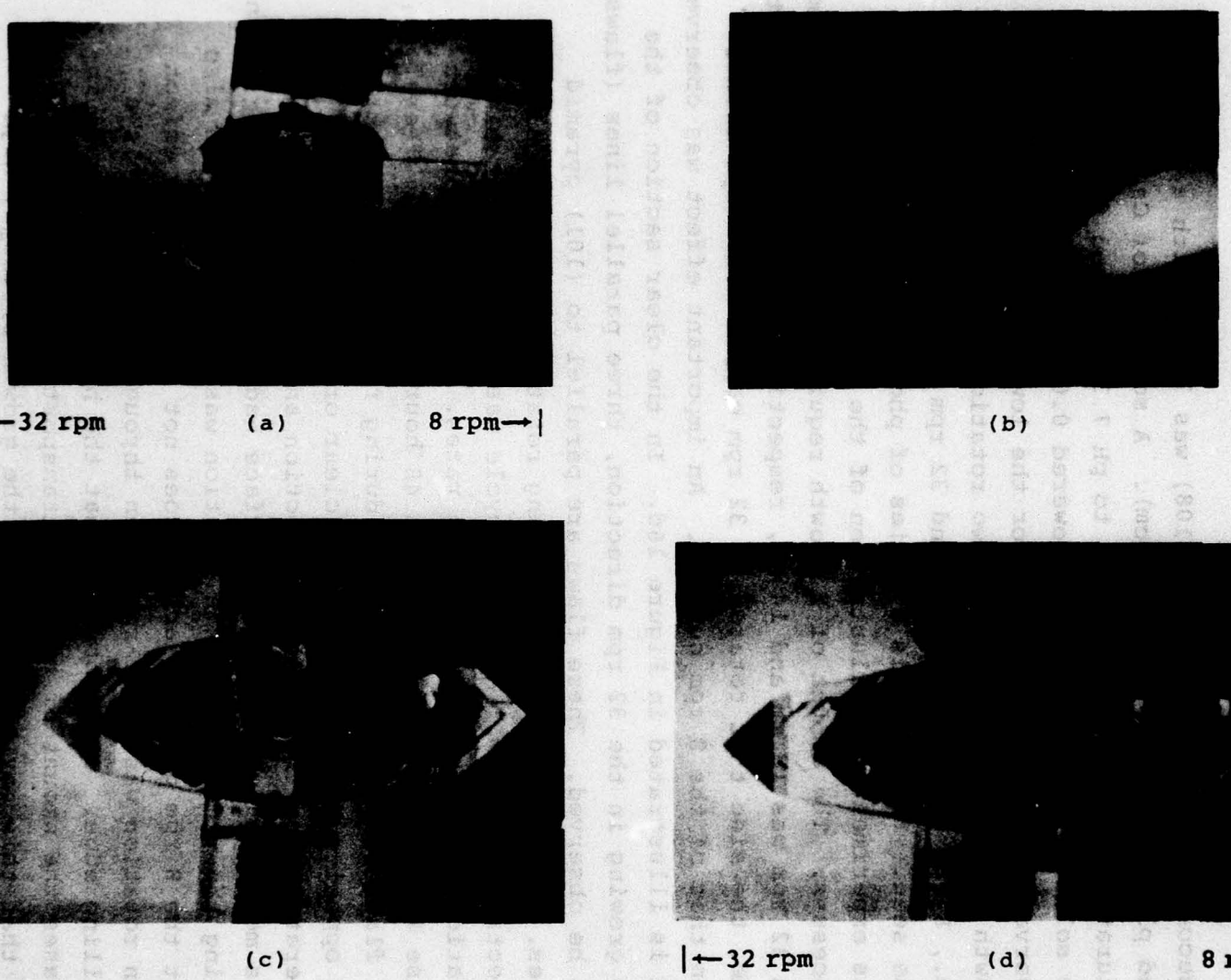

Figure 16: Growth of CsD_2AsO_4 (Run #1-108).

Figure 17 shows the effect of increased rotation rate on the average growth rate in the Z direction for the experiment described. Two points are important. First, the growth rate in the 8 rpm direction is initially slower and this is directly related to a slow capping process at 8 rpm. The second fact, apparent from the data, is that the growth rates at both rotation rates become equal after about 17 days. This corresponds to the time when both growing surfaces have completely capped. It is evident that the growth rate on capped surfaces is equivalent and independent of the rotation rates used in this experiment.

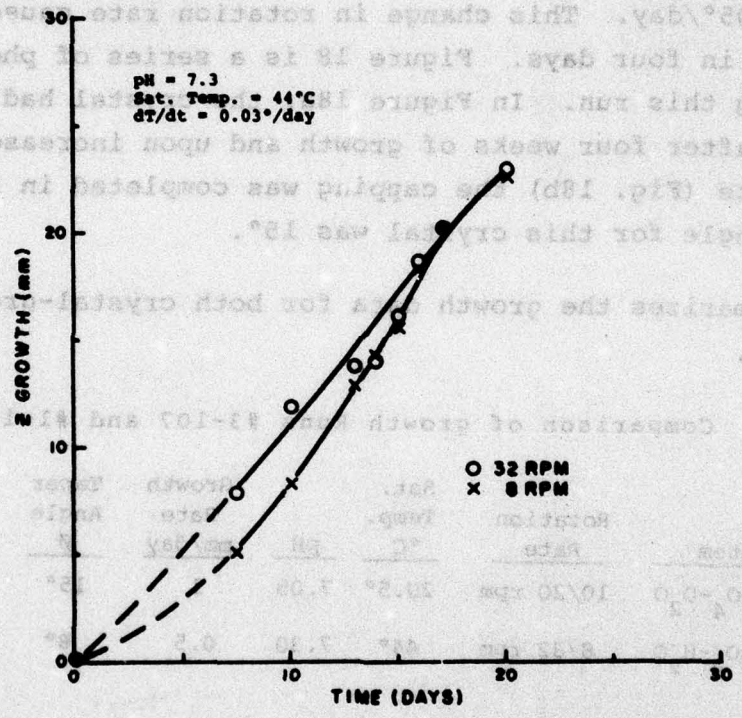

Figure 17: Effect of rotation on growth rate of CsD_2AsO_4.

5.2.4 Low Temperature Growth of CsD_2AsO_4

A low temperature growth Run (#3-107) of CsD_2AsO_4 was initiated based on a comparison of growth data for CsD_2AsO_4 and KD_2PO_4. An extension of the solubility curve of CsD_2AsO_4 in D_2O (by extrapolation) to a solubility value comparable with KD_2PO_4

results in a temperature of -30°C. It was assumed that controlled growth and elimination of many of the CsD_2AsO_4 problems could be achieved by cooling from a saturation temperature of 0° down to approximately -30°C. In order to establish experimentally the validity of these assumptions, Run #3-107 was initiated at 85%D, using a saturation temperature of 20.5°C and pH 7.1. A slow cooling rate (dT/dt) of 0.05°C/day was employed. The crystal had not capped after four weeks of growth. Initially the seed was rotated at 10 rpm and in view of previous indications that increased rotation shortened the capping process, the rotation rate was increased (after four weeks) to 20 rpm and dT/dt remained 0.05°/day. This change in rotation rate caused the seed to cap in four days. Figure 18 is a series of photographs taken during this run. In Figure 18a, the crystal had not capped completely after four weeks of growth and upon increase of the rotation rate (Fig. 18b) the capping was completed in four days. The taper angle for this crystal was 15°.

Table 9 summarizes the growth data for both crystal-growth experiments.

TABLE 9: Comparison of growth Runs #3-107 and #1-108.

System	Rotation Rate	Sat. Temp. °C	pH	Growth Rate mm/day	Taper Angle Ø
CsD_2AsO_4-D_2O	10/20 rpm	20.5°	7.05	1	15°
CsD_2AsO_4-H_2O	8/32 rpm	44°	7.30	0.5	8°

Both crystal growth solutions were prepared from the same purity starting materials; thus the taper angle generated in both of these runs is not impurity dependent. In fact, the effect of impurities on the taper angle appears to be less of a factor than previously observed for KD_2PO_4 (Refs. 16, 17). Figure 19 illustrates the growth rate measured in the Z direction for the #3-107 run. The slope of the curve results in an average growth rate of 1 mm/day with the crystal growth parameters employed. It

(a)

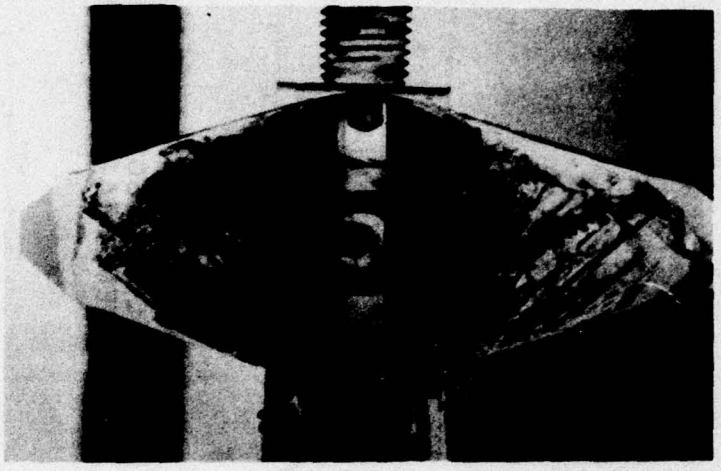

(b)

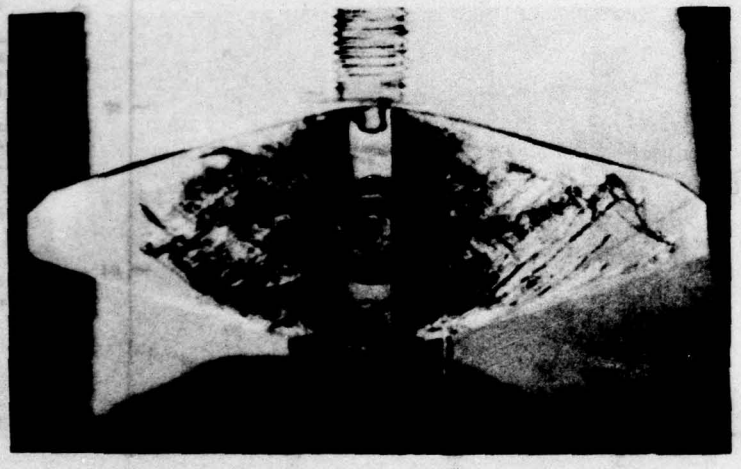

(c)

(d)

Figure 18: Growth of CsD_2AsO_4-D_2O (Run #3-107).

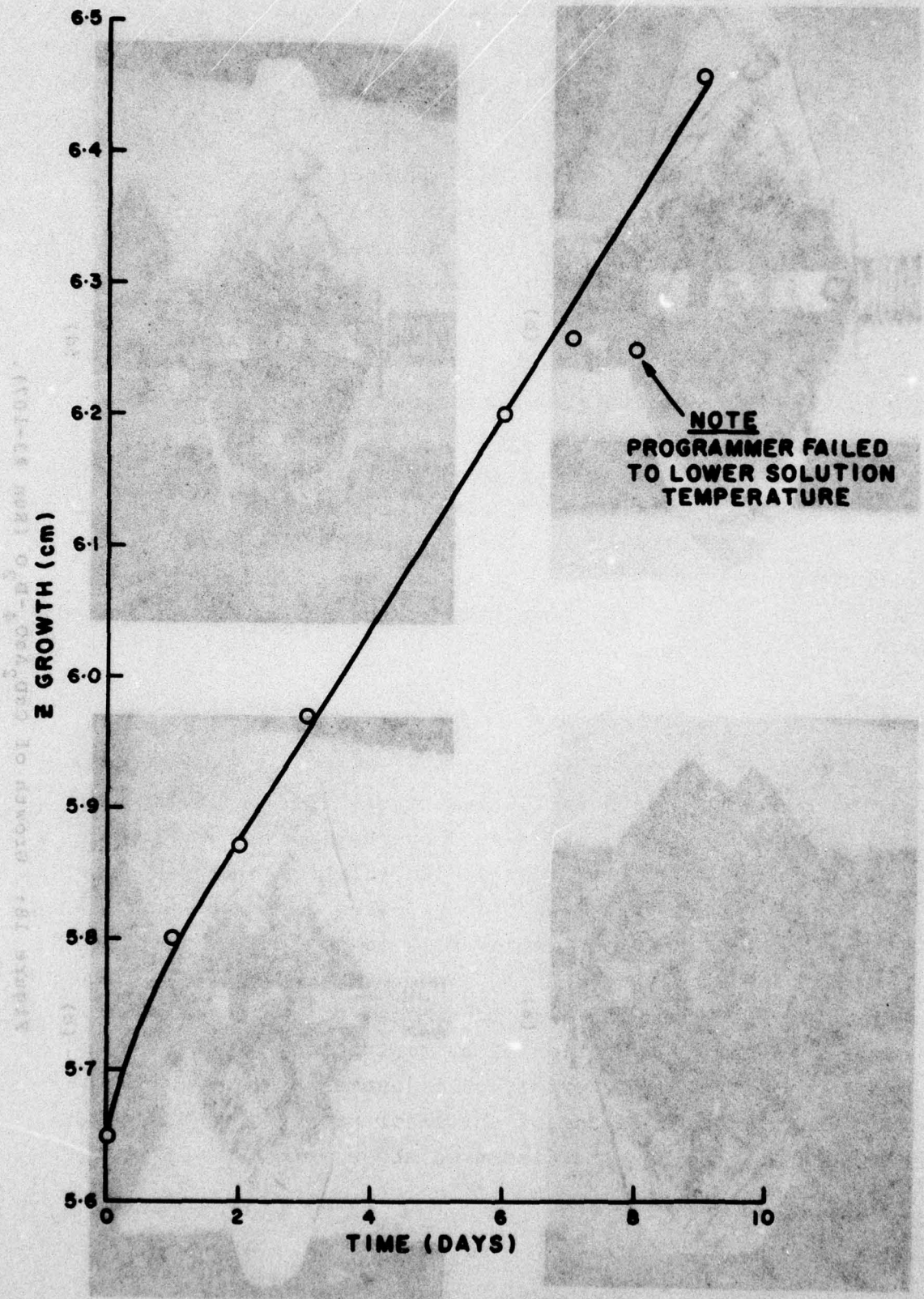

Figure 19: Growth rate of CsD_2AsO_4 (Run #3-107).

should be noted that the data point at 8 days is lower because the temperature did not decrease in the system. The fact that growth stopped would indicate that the growth parameters used in this experiment resulted in a low supersaturation.

This run was terminated due to a malfunction of the temperature controller which caused an increase of 5°C in the growth solution temperature. The result of this temperature rise was a loss of about 50% of the grown crystal.

5.2.5 Effects of Rotation on Capping Process

In view of the apparent dependence of rotation rate on the capping process a modified crystallizer was fabricated. This unit would permit continuous adjustment of fluid flow against the seed surface. Figure 20 illustrates the capping process in the modified crystallizer. The seed never completely capped at rotation rates of 100 rpm. It is not clear at this time if this was due to the high rotation rate or the very poor quality of seed plate utilized.

5.2.6 The Taper Phenomenon

The occurrence of taper in tetragonal KH_2PO_4 crystals has been observed and explained in the literature (Refs. 8,9,10,11). Crystal morphology was influenced by pH, supersaturation (to a minor extent) and foreign cations in solution. In the case of cation impurities, the effect on tapering decreased in the order $Cr^{+3} > Fe^{+3} > Al^{+3}$ and was directly related to the stabilities of the aqua ion complex $M(H_2O)_6^{+3}$ (where M = Cr,Fe,Al). The taper effect in pure solutions was attributed to the corresponding complex formed by hydration of hydronium ions $H_3O\ (H_2O)_3^+$ and could be controlled by proper pH adjustment. In view of the fact that tapering is one of the major problems in the growth of CsD_2AsO_4, the results discussed above were applied to the CsD_2AsO_4-D_2O system.

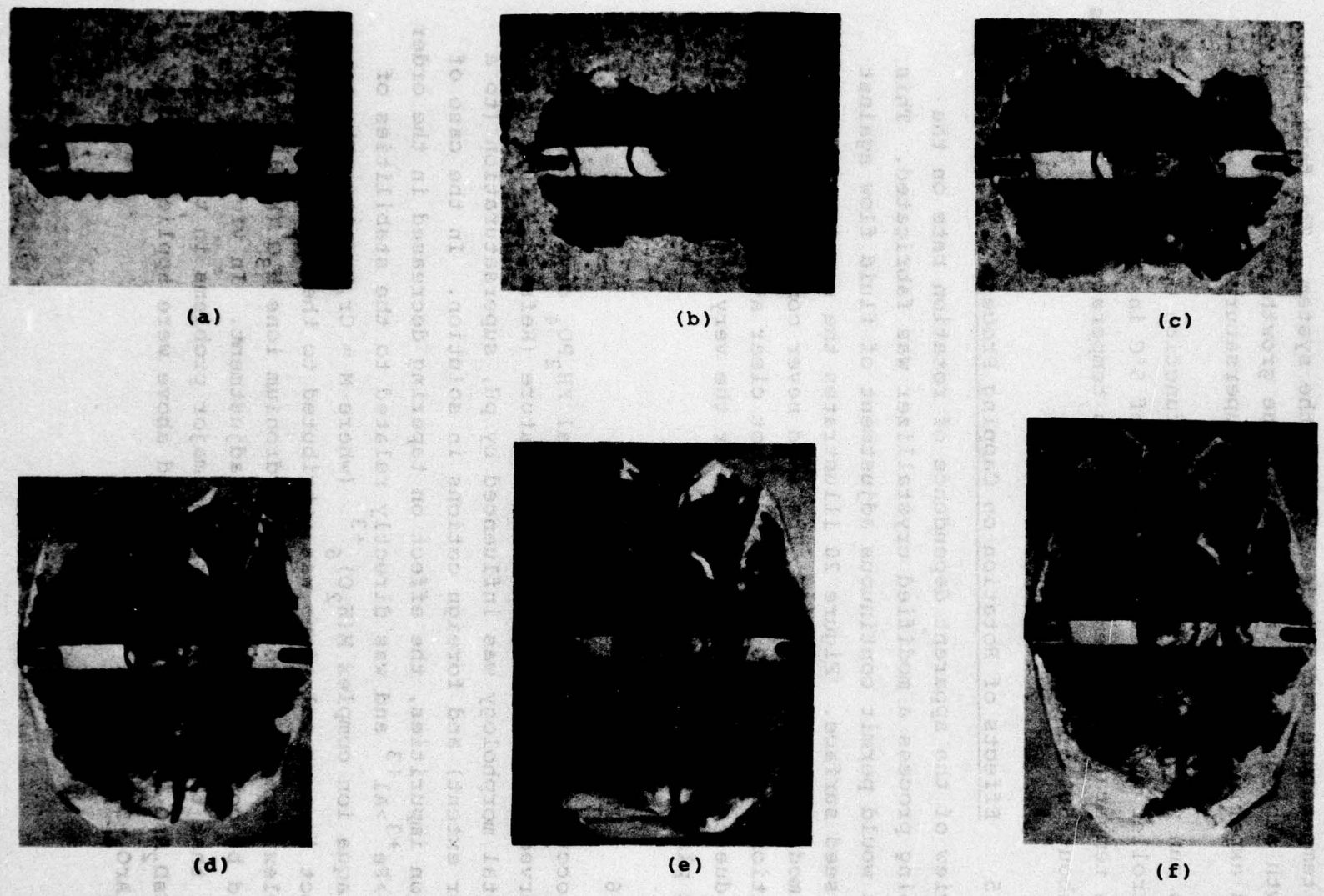

Figure 20: Capping process-turbine experiment (Run # 8-122).

Two impurity additions were selected for incorporation into the CsD_2AsO_4 solutions, Fe^{+3} and BO_3^{-3}. The presence of BO_3^{-3} anions is known to cause tapering $NH_4H_2PO_4$. The solution from Run #3-121 was doped with 500 ppm H_3BO_3 and identified as Run #1-125. A second solution, used previously for Run #8-122, was doped with 300 ppm Fe^{+3} (Run #8-127). Growth conditions for both runs were adjusted to match the runs used with the original undoped solutions (Run #3-121 and 8-122). It should be noted that standard growth solutions contain 5 ppm Fe^{+3} and have resulted in taper angles of 4.5°-15°, thus an increase in Fe^{+3} concentration should result in larger taper angles. Table 10 lists the data obtained from these two runs. For comparison the data from the original solutions are included.

TABLE 10: Growth data for impurity effects

Run #	%D	pH @ 20°C	Impurity Concentration	Taper Angle
3-121	87	7.2	0	7.5°
1-125	87	7.4	500 ppm BO_3^-	13°
8-122	56	7.6	0	13°
8-127	56	7.5	300 ppm Fe^{+3}	13°

There was no observable differences in crystal quality as compared to the undoped experiments. The measured taper angles of the two boules were 13°. There was no change for Fe^{+3} doping and an apparent increase for the BO_3^- experiment. Two conclusions can be inferred from the experiments. First, under the growth conditions used, the addition of Fe^{+3} has no effect on the taper angle in CsD_2AsO_4. Second, the addition of the BO_3^- anion causes an apparent increase in the taper angle but considering the low level of BO_3^- in the standard solutions, this impurity cannot be responsible for the generally observed taper angles in normal CsD_2AsO_4 crystal growth experiments.

The effects of impurities (cation/anion), pH and rotation rate (i.e., fluid flow) on taper in CsD_2AsO_4 are minimal (see Table 11).

TABLE 11: Taper angle data.

Run #	Growth Rate mm/day	dT/dt °/day	Deposition Rate, g/day	Flow Velocity cm/sec.	Taper Angle	pH @20°C	Solution %D*	Deposition Rate Per Unit Area
1-102	--	0.15	3.4	7.2	0°	7.2	68	4.8×10^{-3}
2-103	--	0.08	3.4	4.5	5.5°	6.6	49	7.4×10^{-3}
8-104	--	0.07	7.8	--	6°	6.5	60	21.7×10^{-3}
1-108	2.2	0.06	1.4	11.4 2.9	6°	7.3	0	3.6×10^{-3}
8-115	--	0.30	21.5	16.2	4.5°	8.1	96	74.6×10^{-3}
8-120	1.8	0.19	3.2	16.2	10.5°	7.8	85	9.1×10^{-3}
3-121	1.0	0.23	1.6	16.2	7.5°	7.2	87	3.3×10^{-3}
8-122	3.0	0.30	6.1	--	13°	7.6	56	6.8×10^{-3}
1-123	3.4	0.15	5.6 2.3	19.5 13.8	14° 10°	7.6	56	10.2×10^{-3} 5.9×10^{-3}
5-133	1.2	0.10	1.0	16.2	0°	7.2	?	3×10^{-3}

Initial data on pH and rotation rates indicate, that while these two parameters do have some effect on the taper angle, there is insufficient data to explain the continued existence of a finite, variable taper angle. In the case of pH, it was noted that CsD_2AsO_4 solutions initially prepared at pH 4.1 had changed on standing, to pH 2.6. One possible explanation for this behavior is the presence of CO_2 in solution. During the preparation of CsD_2AsO_4, Cs_2CO_3 is used as a starting component and CO_2 is produced during the neutralization process:

$$Cs_2CO_3 + 4D_2O + As_2O_5 \overset{D_2O}{\rightleftharpoons} 2CsD_2AsO_4 + 2D_2O + CO_2\uparrow \quad (1)$$

The CO_2 generated could then react as shown below:

$$CO_2 + D_2O \rightleftharpoons D_2CO_3 \quad (2)$$

$$2D_2CO_3 + Cs_2CO_3 \rightleftharpoons 2CsDCO_3 + CO_2 + D_2O \quad (3)$$

The presence of CO_2 in the solution could lead to aqua complexes of the type described above and therefore lead to tapering. To investigate this aspect of the taper problem, solution Run

#3-121 was refluxed for 72 hours (the final $[CO_2]$ being <100 ppm) and subsequently used for a crystal growth run (#3-124). The taper angle on this crystal was 9°, very close to the taper angle of Run #3-121 (7.5°). During the growth run, the solution pH was monitored over an eight hour period and did not vary: pH 7.596 $\pm$ 0.002. Thus CO_2 in solution is not responsible for taper under the conditions employed.

Another possible source of taper in CsD_2AsO_4 could be Rb^+ contamination. While it appeared unlikely that Rb^+ could result in taper, it was noted that RbH_2AsO_4 seed plates in a CsD_2AsO_4 solution resulted in dendritic growth. A chemical analysis of two crystals, with 14° taper and 0° taper showed the Rb^+ concentration to be 10 and 20 ppm, respectively. Rb^+ was therefore eliminated as a possible source.

CsD_2AsO_4 crystallization from a stoichiometric aqueous solution can be described chemically by the following reactions.

$$CsD_2AsO_4 \rightleftharpoons Cs^+ + D_2AsO_4^- \quad (4)$$

$$D_2AsO_4^- \rightleftharpoons D^+ + DAsO_4^{-2} \quad (5)$$

$$D_2O \rightleftharpoons D^+ + OD^- \quad (6)$$

$$D^+ + D_2AsO_4^- \rightleftharpoons D_3AsO_4 \quad (7)$$

$$CsOD \rightleftharpoons Cs^+ + OD^- \quad (8)$$

$$Cs^+ + DAsO_4^{-2} \rightleftharpoons CsDAsO_4^- \quad (9)$$

These equations are representative of a number of possible processes. Assuming Cs^+ and $D_2AsO_4^-$ ions form chains along the [001] axis as previously described for RbH_2PO_4 (Ref. 10), the (100) face consists of both ions. The (100) face contains alternating planes of Cs^+ and $D_2AsO_4^-$. This is recognized to be a simplification of the actual system because $D_2AsO_4^-$ is actually $D_{2-x}H_xAsO_4^-$. The lack of one ion would cause a change in growth habit: i.e., D^+ in

excess should cause elongated growth. In a stoichiometric solution (pH 4.6) Equation (5) is negligible. Addition of CsOD would increase the pH and result in excess Cs^+ which would promote reaction (9). Then, the total D_2AsO_4 concentration would decrease. Under these conditions the formation of $D_2AsO_4^-$ layers on (001) faces would be delayed and taper results. Thus, theoretically crystal growth at pH 4.6 should result in taper-free crystals. This has not been the case of previous data and present results showed taper exists over the entire pH range 4 to 8 (Ref. 1).

The interfacial angles of a tapered CsD_2AsO_4 crystal were measured with a precision protractor. Since the faces are curvilinear, the angle ϕ ranged from 24° to 28°. A 3 mm^3 chip, exhibiting the taper surface was analyzed on the X-ray precession camera. The surface of the chip was aligned and auto-collimated to the spindel and X-ray beam directions. The precession diagrams confirm the crystallographic orientations shown in Figure 21. The set of planes which closely correspond to the taper

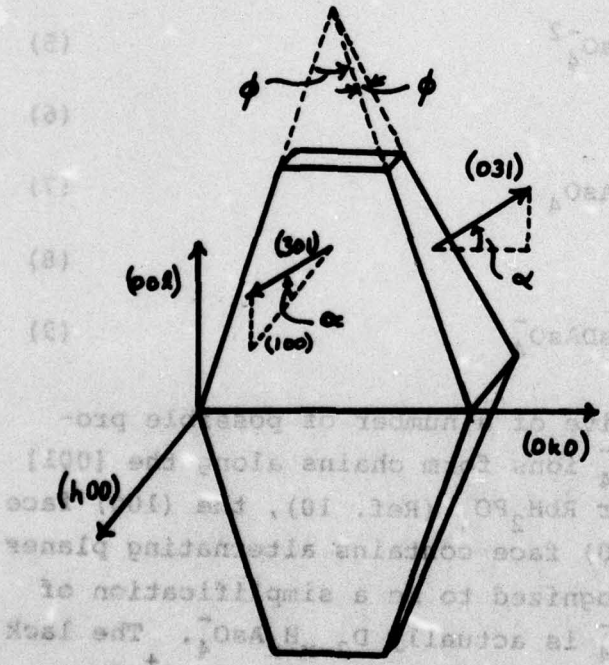

Figure 21: Orientation of tapered CsD_2AsO_4 crystal.

faces were the {301}. The misorientations between these faces and crystallographic planes vary from 2° to 4°.

Table 11 summarizes the data from the various crystal growth runs with specific reference to the taper problem. No correlation between taper angle and growth parameters could be clearly established.

Table 12 summarizes the total impurities analysis for a typical tapered boule and its growth solution. No correlation is obvious between taper angle and impurity concentrations.

TABLE 12: Quantative analysis of typical tapered CsD_2AsO_4 crystal and growth solution

Impurity	Solution (ppm)	Crystal * (ppm)
Na	5	5
K	10	---
Rb	2	2
B	5	1
Al	5	1
Si	10	1
Mg	5	1
Ca	10	1
Cu	50	---
Tl	10	---
P	10	60
CO_2	<50	---

* --- Sought but not detected. In addition, Fe, Ba, Be, Mn, Pb, Cr, Ag, Sn, Th and V were not detected.

5.2.7 Growth Process for Taper-Free CsD_2AsO_4

During an analysis of all crystal growth data obtained under this program, an interesting phenomenon was observed. In early crystal growth runs using glycol/D_2O (70:30) as a solvent, the taper angle in CsD_2AsO_4 appeared to be less than 5°. However,

the 0°Z plates used as seeds never completed the "capping process". In addition, crystal growth was highly flawed as evidenced by a high concentration of growth veils. Therefore, it was decided that a previously capped and tapered crystal introduced into a saturated CsD_2AsO_4-glycol/D_2O solution might grow with a reduced taper angle.

A CsD_2AsO_4 growth solution was prepared using glycol/D_2O (70:30) at pH 7.55 and a saturation temperature of 46.5°C. Final solution volume was 2.1 liters. The capped boule with a taper angle of 16°, grown in Run #1-125 (BO_3^{-3} doped), was used as the seed. A constant rotation of 60 rpm was maintained during the entire growth process. The temperature lowering rate was 0.2°/day. Figure 22 illustrates the growing CsD_2AsO_4 crystal 14 days into

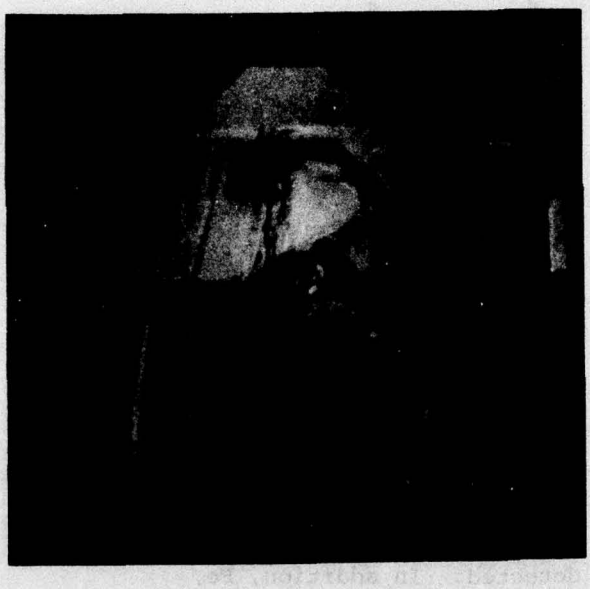

Figure 22: CsD_2AsO_4 crystal (Run #1-129) [Sat. temp. 46.5°C, pH 7.55, 60 rpm, dT/dt = 0.2°/day].

the cycle. The internal flaw observed is the initial boundary of the seed crystal. Allowing for magnification, about 3.5 mm of clear crystal growth was observed at the cap, measured perpendicular to the Z axis. Thus, the taper angle was reduced from 16° to about 6°. It would appear that a two step process could be used to grow large optical quality CsD_2AsO_4.

A second crystal growth run (#5-133) was initiated at the end of this program and the resulting crystal (in situ) is shown in Figure 23. For comparison, the crystal from Run #1-129 is also shown.

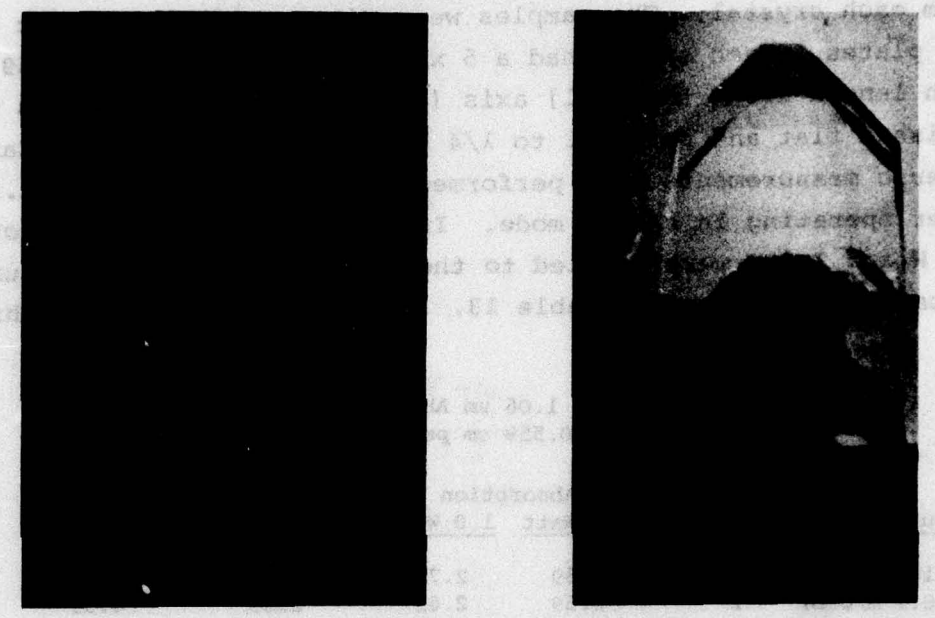

(a) Run #1-129 (b) Run #5-133

Figure 23: CsD_2AsO_4 growth.

SECTION VI

CRYSTAL CHARACTERIZATION

6.1 Optical Absorption Measurements

Three CsD_2AsO_4 crystals were grown at solution deuteration levels of 48.7, 59.9 and 68.2% D, and three test samples were fabricated from each crystal. The samples were X-ray oriented and cut as 0°Z plates. Each sample had a 5 x 5 mm aperature and a 5.59 mm path length along the [001] axis (Z). Opposite (001) faces were polished flat and parallel to $\lambda/4$ and 20 seconds of arc. Calorimeteric measurements were performed using the output of a 1.06 μm laser operating in the CW mode. Input powers (at 1.06 μm) of 0.3 W and 1.0 W were applied to the test samples. The measurements are summarized in Table 13. Figure 24 is a plot of this

TABLE 13: 1.06 μm Absorption in CsD_2AsO_4 (0.559 cm path length [001])

Boule #	Sample #	% Absorption 0.3 Watt	% Absorption 1.0 Watt	Mean Absorption	Absorption % per cm
2-103	1	2.59	2.77		5.4
(48.7 m/o D)	2	2.59	2.62	2.59	4.59
	3	2.52	2.44		
8-104	1	2.20	2.24		
(59.9 m/o D)	2	2.39	2.30	2.27	4.02
	3	- Broken -			4.4
1-102	1	1.45	1.42		
(68.2 m/o D)	2	1.22	1.18	1.29	2.30
	3	1.22	1.23		3.2

data together with two measurements obtained from the literature for 0% and 85% D (Ref. 4, 5). Neither of the literature values were made by the calorimetric method. The deuteration levels indicated at 0% and 85% are those measured in the crystals. Figure 24 shows that deuterations higher than 85% (in the crystal) are required to obtain absorption in the 0.5%/cm region. The same crystals were also measured in the 45°Z SHG direction and gave the following absorptions: Run #2-103: 7.4% per cm; Run #8-104: 6.0% per cm; and Run #1-102: 6.2% per cm.

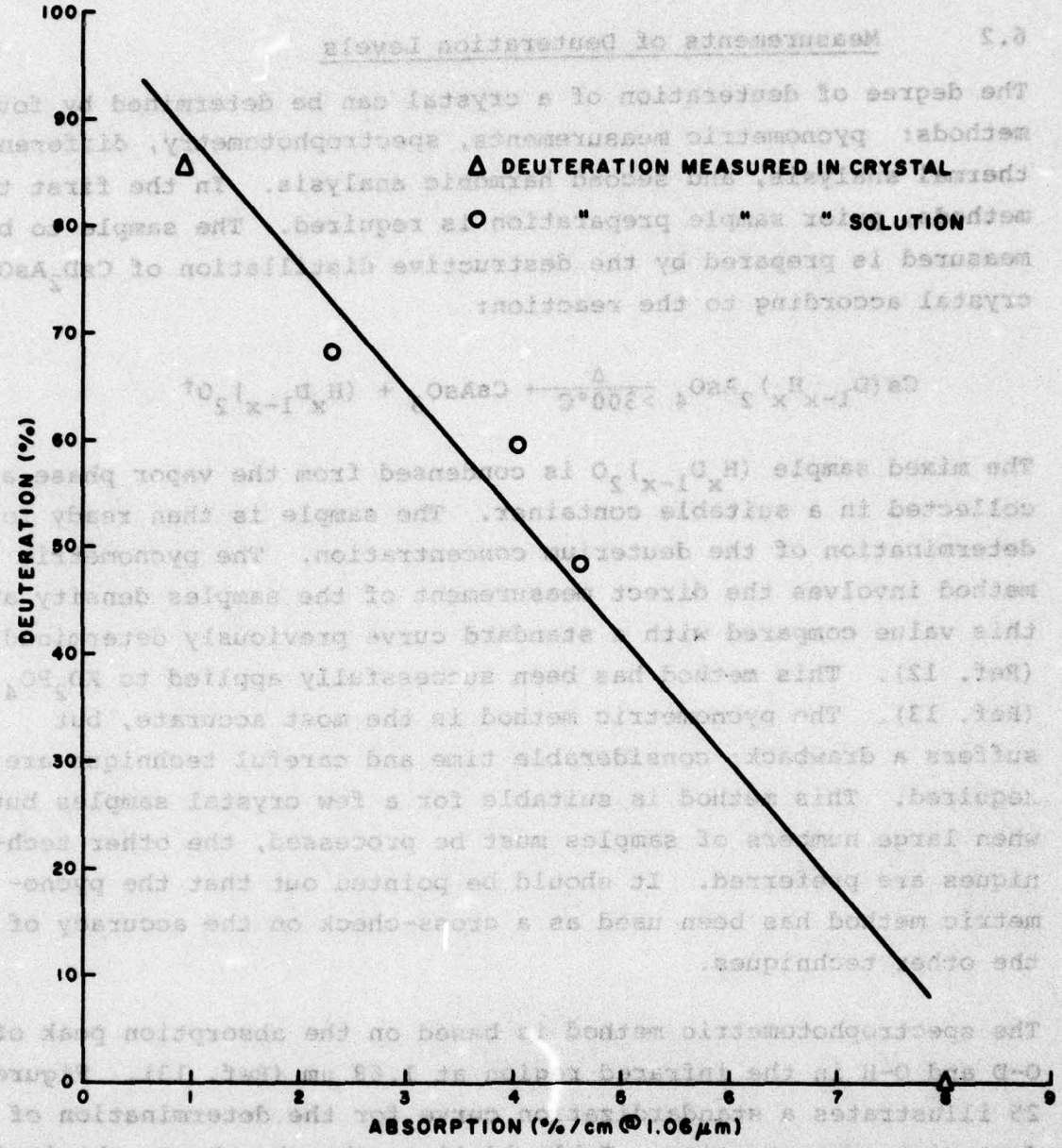

Figure 24: Optical absorption in CsD_2AsO_4 at 1.06 μm.

The consequence of this high deuteration level requirement is discussed in Paragraphs 6.3 and 6.4, in relation to the phase match temperature and to a recently discovered phase transition in CsD_2AsO_4.

6.2 Measurements of Deuteration Levels

The degree of deuteration of a crystal can be determined by four methods: pycnometric measurements, spectrophotometry, differential thermal analysis, and second harmonic analysis. In the first two methods, prior sample preparation is required. The sample to be measured is prepared by the destructive distillation of CsD_2AsO_4 crystal according to the reaction:

$$Cs(D_{1-x}H_x)_2AsO_4 \xrightarrow[>300°C]{\Delta} CsAsO_3 + (H_xD_{1-x})_2O\uparrow$$

The mixed sample $(H_xD_{1-x})_2O$ is condensed from the vapor phase and collected in a suitable container. The sample is then ready for determination of the deuterium concentration. The pycnometric method involves the direct measurement of the samples density and this value compared with a standard curve previously determined (Ref. 12). This method has been successfully applied to KD_2PO_4 (Ref. 13). The pycnometric method is the most accurate, but suffers a drawback; considerable time and careful technique are required. This method is suitable for a few crystal samples but when large numbers of samples must be processed, the other techniques are preferred. It should be pointed out that the pycnometric method has been used as a cross-check on the accuracy of the other techniques.

The spectrophotometric method is based on the absorption peak of O-D and O-H in the infrared region at 1.68 μm (Ref. 13). Figure 25 illustrates a standardization curve for the determination of deuterium concentration. Table 14 lists the absorbance obtained for a particular mole percent deuterium level. The technique uses a pair of matched path-length quartz cells. Again, a direct measurement is performed on the distilled sample and the concentration of deuterium determined from the standard curves. It should be noted that to retain accuracy and reproducibility of the measurements, standard samples should be available during the testing of unknowns and periodic checks performed.

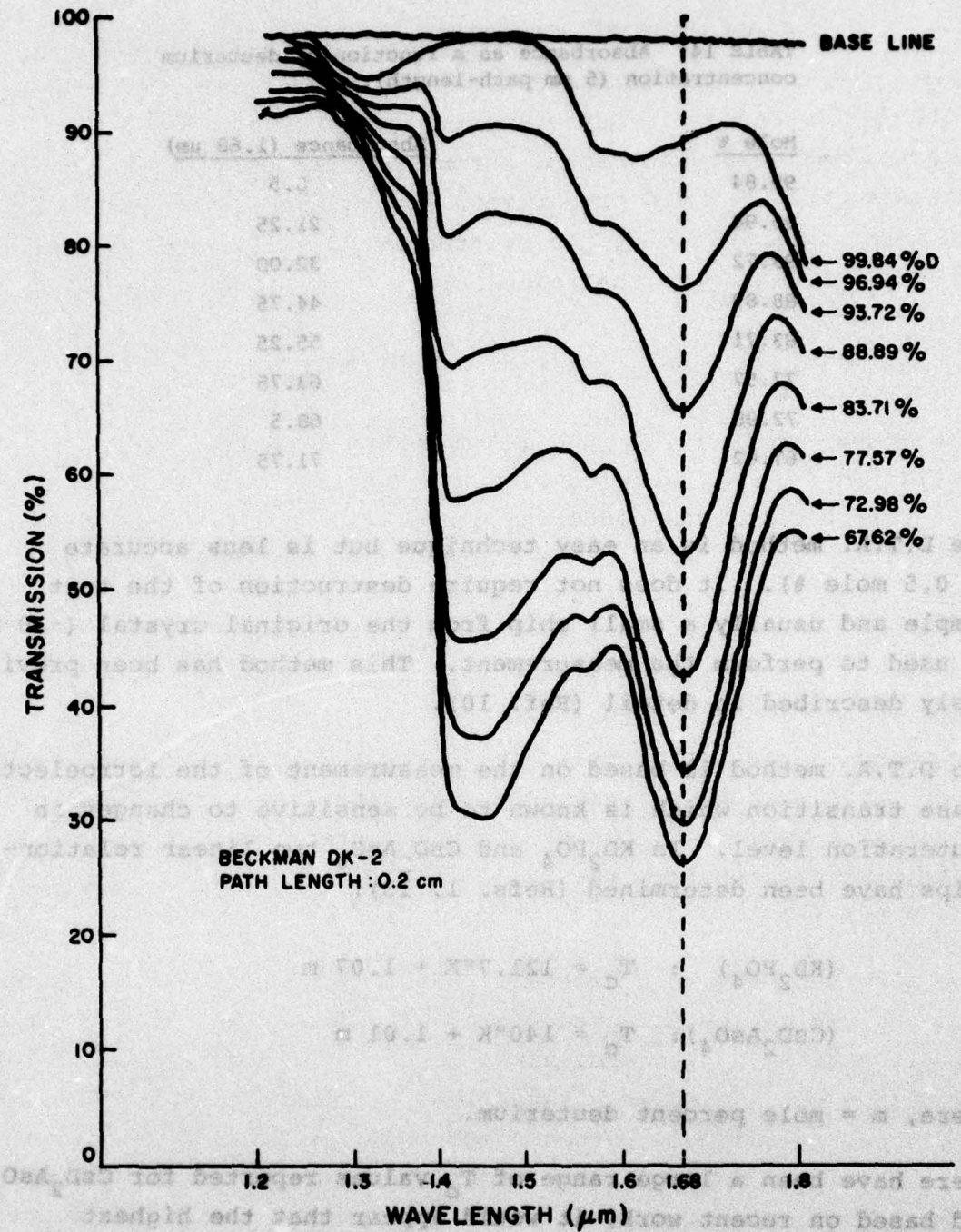

Figure 25: Standardization curves for deuteration levels.

TABLE 14: Absorbance as a function of deuterium concentration (5 mm path-length).

Mole %	Absorbance (1.68 μm)
99.84	8.5
96.94	21.25
93.72	32.00
88.89	44.75
83.71	55.25
77.57	63.75
72.98	68.5
67.62	71.75

The D.T.A. method is an easy technique but is less accurate (± 0.5 mole %). It does not require destruction of the test sample and usually a small chip from the original crystal (~10 mg) is used to perform the measurement. This method has been previously described in detail (Ref. 10).

The D.T.A. method is based on the measurement of the ferroelectric phase transition which is known to be sensitive to changes in deuteration level. In KD_2PO_4 and CsD_2AsO_4 two linear relationships have been determined (Refs. 1, 13):

$$(KD_2PO_4) \quad : \quad T_c = 121.7°K + 1.07\ m$$

$$(CsD_2AsO_4): \quad T_c = 140°K + 1.01\ m$$

where, m = mole percent deuterium.

There have been a large range of T_c values reported for CsD_2AsO_4 and based on recent work, it would appear that the highest deuterated crystal was only just obtained (Ref. 1). A major point to be considered is the lack of data on the distribution coefficient (k_{eff}) of deuterium for CsD_2AsO_4. Previous work has shown that in KD_2PO_4, k_{eff} is not unity (Ref. 13). In CsD_2AsO_4, the only reported measurement is 85.6% in the crystal, which was grown

from a 93% solution. The distribution coefficient in this case is therefore, $k_{eff} = 0.92$ but, as in the case of KD_2PO_4, its value will vary as a function of deuterium concentration in the growth solution and as a function of the pH. The average effective distribution coefficient of D* in CsD_2AsO_4 over the range of solution concentrations (49-68%) was calculated as 0.87 ± 0.02.

6.3 Measurement of Phase Match Temperature (T_{pm})

Three samples of CsD_2AsO_4 with different deuteration levels were used to measure T_{pm}. These crystals were the same as those used for the optical absorption measurements (Runs #2-103, #8-104, and #1-102). Table 15 lists the values obtained for doubling of the 1.06 μm laser.

Figure 26 illustrates the plotted data. Based on this data and the optical absorption values shown in Figure 24, to obtain CsD_2AsO_4 with optical absorption less than 0.5%/cm would require a [D*] crystal of ~95%. The resulting 90° phase match temperature would exceed 410 °K (137°C). It is assumed that the difference in absorption are due only to variations in crystal deuteration levels.

TABLE 15: T_{pm} values for various deuterations.

Crystal	$[D^*]_{crystal}$ (†)	T_{pm} °C	Remarks
2-103	43	70° ± 2°	narrow SHG peak
8-104	51	80° ± 2°	broad peak
1-102	61	77° ± 2°	broad peak
Ref. 1	85	116° ± 5°	

(†) Calculated from Curie temperature measurements.

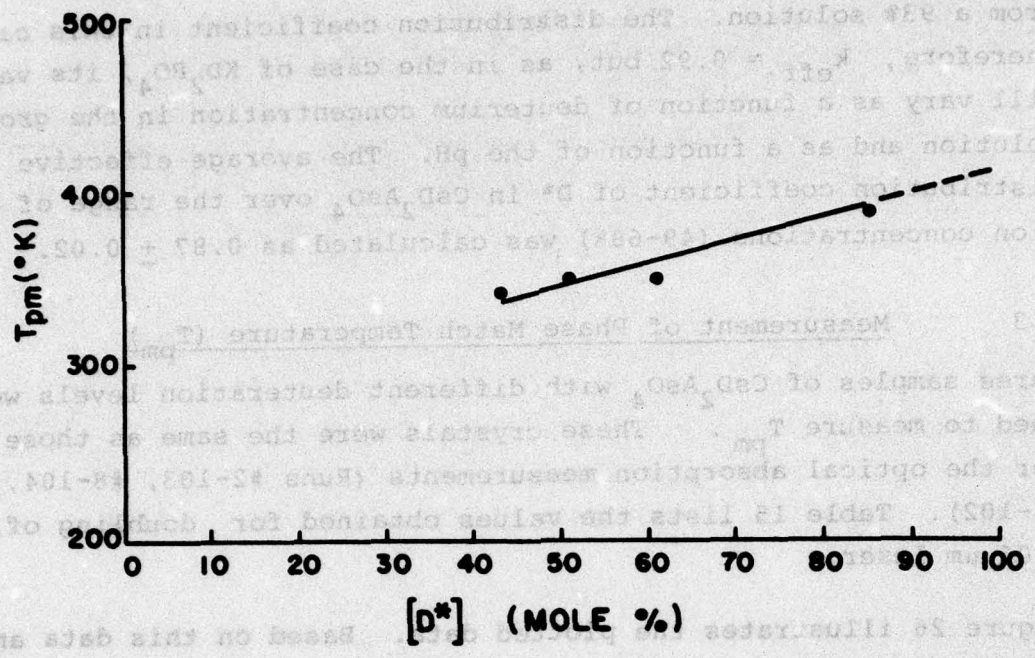

Figure 26: 90° phase match temp. vs. [D*] crystal.

6.4 Thermal Stability and Phase Transitions in CsD_2AsO_4

The thermal stabilities of KH_2PO_4 type crystals were recently reported (Ref. 14). The onset of weight loss was considered to be the start of decomposition and for CsD_2AsO_4; this transition occurs at 469°K. This value is considered an upper limit for the thermal stability. In addition, loss of transparency occurs before this temperature is reached.

There are a total of three phase transitions in CsD_2AsO_4. Two of these transitions are predicted from the double minimum potential well theory of hydrogen bonded ferroelectric and are associated with the ferroelectric-paraelectric transition (227°K) and the decomposition temperature (469°K) of CsD_2AsO_4. A third transition has been discovered at 443°K which is destructive (Ref. 15). This transition is associated with a change in crystal structure from tetragonal to monoclinic and has also been observed to occur in other KH_2PO_4 type crystals. Table 16 lists the interplanar spacings, peak intensities and lattice parameters for the high temperature phase of CsD_2AsO_4. It should be noted that D.T.A. data indicates the onset of this transition occurs at 409°K.

TABLE 16: Interplanar spacings and peak intensity (I_p) of high temperature phase of $Cs(D_{0.85}H_{0.14})_2AsO_4$.

H	K	L	D(obs)	D(calc)	I_p
0	1	3	3.7538	3.7538	1500
3	0	2	3.4395	3.4395	500
$\bar{3}$	1	0	3.3066	3.3066	500
$\bar{4}$	0	0	2.9746	2.9746	400
1	1	5	2.5363	2.5308	400
$\bar{3}$	2	0	2.3881	2.3854	800
5	0	2	2.2444	2.2438	200
2	2	4	2.1373	2.1384	500
$\bar{4}$	2	2	2.0367	2.0351	150
$\bar{4}$	1	5	1.9876	1.9857	500
5	0	4	1.9617	1.9646	500
5	2	1	1.8415	1.8418	150
$\bar{6}$	0	4	1.7620	1.7618	150
$\bar{4}$	3	1	1.6480	1.6487	500
$\bar{7}$	0	3	1.6170	1.6187	200
$\bar{4}$	3	4	1.5157	1.5154	500
$\bar{1}$	4	1	1.4765	1.4764	500
2	1	10	1.3621	1.3622	125
8	2	3	1.2736	1.2750	500

$a_o = 11.89$ Å; $b_o = 5.98$ Å; $c_o = 14.51$ Å; $\beta = 91.7°$; Vol. $= 1031$ Å^3

SECTION VII
CONCLUSIONS

The behavior of the CsD_2AsO_4 crystal growth process has still not been completely explained. Data obtained during this program has increased the insight required to formulate a viable crystal growth process and has resulted in an empirical process where CsD_2AsO_4 can be grown with a mimium taper angle (Par. 5.2.7). It was established that the following parameters do not have an appreciable effect on taper:

- pH in the range 6.5 - 8.1.
- Impurity content of starting materials.
- Deposition rate.
- Temperature lowering rate.
- Rotation rate (solvent flow velocity).
- Solution [D*].
- Solvent composition.
- Seed holder configuration.

The program also underscored the importance of high-quality seed crystals and the problems involved with their growth. Indications are that the conditions required for seed growth and, in particular, to the generation of larger seed cross-section, i.e., X-Y growth, are not suited for bulk crystal growth. Further work to define these conditions is required. It was also concluded that unless a method for growing high-quality seed material is established, the growth of large, high-optical-quality CsD_2AsO_4 will not be possible. Furthermore, a considerable amount of uncertainty exists regarding the effect of seed quality on other CsD_2AsO_4 parameters, i.e., absorption, taper, deuteration uniformity, etc.

The results of the study of the mixed solvent system D_2O/glycol concluded that a decrease in association of the growth solution did not occur. Furthermore, a large number of additional solvents (non-aqueous) were screened but none were found suitable for the growth of tetragonal CsD_2AsO_4. The solubility data for these mixed solvents also illustrated the unstable nature of these systems.

The discovery of a third phase transition in CsD_2AsO_4 associated with a structural change from tetragonal to monoclinic at 409°K will have a significant impact on the future utility of CsD_2AsO_4. The need for low absorption crystals (at 1.06 μm) will require a trade-off in optimum properties for CsD_2AsO_4. For example, if 0.5%/cm is desired, the crystal deuteration level will have to approach 95 mole %. This in turn will increase the 90° phase match temperature to 410°K--which is where the destructive phase transition is initiated. Methods other than adjustment of deuteration levels will have to be examined to reduce optical absorption. One possibility could be the improvement of the seed material.

A number of interesting crystal growth parameters were examined during this program and the following observations made:

- Growth in D_2O/glycol solvent increases tendency of crystal to flaw.
- pH stability (range 6-7) in D_2O during growth runs is excellent when saturation temperatures are about 40°C.
- Above 50°C the pH of a stoichiometric solution (D_2O) varies by about $\pm$ 0.5 units.
- The trailing face of a crystal in D_2O/glycol will grow at the same rate as the leading face without generating flaws.
- The use of 45°Z plates did not result in improved growth.
- CsH_2AsO_4 could be used as seed material.
- Impurities had minimal effects on taper.
- Increased rotation in D_2O solvent results in shorter capping periods.
- Growth rates up to 5 mm/day can be used without causing visible flaws.
- A taper-free crystal can be grown by first capping a seed plate in D_2O and then using this crystal as a seed for subsequent growth in D_2O/glycol (70:30).

It is clear from the results of the program that more work is needed before a commercially viable CsD_2AsO_4 process can be realized. Due to the amount of time required to grow crystals from solution, a concentrated effort might yield the desired process in two years.

SECTION VIII
RECOMMENDATIONS

The present program has illustrated the need for more information on the growth process of CsD_2AsO_4. Additional studies are clearly indicated. The following are recommended areas of investigation:

- Generation of X-Y growth to develop larger seed cross section.
- Effects of crystal imperfections on optical absorption and phase match temperature.
- Effects of other seed orientations on growth habit.
- Experimental growth of CsD_2AsO_4 in a constant-temperature, three-zone crystallizer similar to the Walker-Kohman unit used to grow $NH_4H_2PO_4$ back in 1948.
- Systematic search for other pure or mixed solvent systems that will reduce the high solubility of CsD_2AsO_4 and still yield tetragonal crystals.

SECTION IX
REFERENCES

1. J. F. Balascio and G. M. Loiacono, Final Report (ONR), Contract No. N00014-73-C-0372 (1974).
2. J. F. Balascio, G. M. Loiacono, S. C. Hayden, and A. Idelson, Mat. Res. Bull. 10, 193 (1975).
3. J. H. Boyden, E. G. Erickson, J. E. Murray, and R. Webb, Final Technical Report (ONR), Contract No. N00014-71-C-0044 (1971).
4. D. T. Hon, IEEE J. Quan. Elec. QE-12, 148 (1976).
5. K. Kato, IEEE J. Quan. Elec. QE-8, 616 (1974).
6. A. Ferrari, M. Nardelli, and M. Cingi, Gazz. Chem. Ital. 86, 1174 (1956).
7. Landolt-Bornstein Tables, Vol. 3 Group III, p. 136, Springer-Verlog, Berlin (1969).
8. H. E. Buckley, Crystal Growth, John Wiley & Sons, Inc., N.Y., 1961.
9. R. J. Davey and J. W. Mullin, J. Cryst. Growth 23, 89 (1974).
10. M. Removisseney, M. Desvignes, and V. Marecek, Krist. un Tech. 5, (4)535 (1970).
11. J. W. Mullin, A. Amatavivadhana, and M. Chakraborty, J. Appl. Chem. 20, 153 (1970).
12. L. Silverman and W. Bradshaw, Anal. Chem. Acta. 10, 68 (1954).
13. G. M. Loiacono, J. F. Balascio, and W. N. Osborne, Appl. Phys. Let. 24, 455 (1974).
14. P. K. Gallagher, Thermochimica Acta. 14, 131 (1976).
15. G. M. Loiacono, J. Ladell, W. N. Osborne, and J. Nicolosi, Ferroelectrics, 11 (1976), to be published.
16. G. M. Loiacono, Acta Elect.
17. V. Marecek, L. Dobiasova and J. Novak, Krist. un Tech. 4, 39 (1969).

APPENDIX A

SAMPLE D-110 CD*A 7/2/75 TETRAGONAL

H	K	L	D(O)	D(C)	D*(O)	PEAK	A*	B*	C*
1	0	1	5.6184	5.6118	0.2742	118.5	0.19302		0.19520
*	*	*	4.4167		0.3488	149.4	0.19302		0.19520
2	0	0	3.9921	3.9906	0.3859	4756.8	0.19302		0.19520
*	*	*	3.5810		0.4302	308.8	0.19301		0.19520
1	1	2	3.2331	3.2341	0.4765	7750.1	0.19300		0.19520
*	*	*	3.2128		0.4795	235.5	0.19301		0.19523
2	2	0	2.8215	2.8220	0.5460	2408.6	0.19301		0.19523
2	0	2	2.8077	2.8057	0.5487	178.1	0.19302		0.19523
3	0	1	2.5210	2.5211	0.6111	572.3	0.19302		0.19523
1	0	3	2.4977	2.4982	0.6168	556.4	0.19302		0.19523
*	*	*	2.3527		0.6548	262.5	0.19302		0.19523
3	1	2	2.1267	2.1261	0.7244	6690.7	0.19302		0.19523
2	1	3	2.1176	2.1177	0.7275	844.7	0.19298		0.19522
4	0	0	1.9953	1.9958	0.7721	695.2	0.19298		0.19522
0	0	4	1.9731	1.9729	0.7808	579.8	0.19299		0.19521
*	*	*	1.9575		0.7870	110.1	0.19299		0.19521
4	1	1	1.8794	1.8803	0.8197	282.4	0.19299		0.19521
4	2	0	1.7851	1.7849	0.8630	1462.4	0.19300		0.19521
4	0	2	1.7779	1.7809	0.8665	90.6	0.19299		0.19521
2	0	4	1.7693	1.7686	0.8707	2255.7	0.19299		0.19521
3	3	2	1.6991	1.6983	0.9067	1971.5	0.19300		0.19516
3	2	3	1.6939	1.6942	0.9095	222.4	0.19297		0.19516
2	2	4	1.6177	1.6173	0.9523	1531.3	0.19297		0.19516
*	*	*	1.6103		0.9567	209.9	0.19297		0.19514
1	0	5	1.5489	1.5489	0.9946	188.3	0.19297		0.19514
*	*	*	1.4650		1.0516	93.1	0.19297		0.19514
5	1	2	1.4556	1.4554	1.0584	2684.6	0.19297		0.19514
2	1	5	1.4442	1.4440	1.0667	107.0	0.19296		0.19515
4	4	0	1.4113	1.4114	1.0916	456.5	0.19296		0.19514
4	0	4	1.4033	1.4034	1.0978	1380.2	0.19296		0.19514
3	3	4	1.3607	1.3619	1.1322	122.0	0.19296		0.19515
6	0	0	1.3305	1.3306	1.1579	359.5	0.19296		0.19515
4	2	4	1.3241	1.3239	1.1635	1800.1	0.19296		0.19515
5	3	2	1.2937	1.2936	1.1908	1223.1	0.19296		0.19514
3	2	5	1.2857	1.2856	1.1982	82.1	0.19296		0.19515
1	1	6	1.2817	1.2814	1.2020	1079.3	0.19296		0.19514
6	2	0	1.2623	1.2623	1.2204	552.5	0.19296		0.19513
3	1	6	1.1669	1.1669	1.3202	1123.0	0.19296		0.19513
4	4	4	1.1482	1.1481	1.3417	352.5	0.19296		0.19512
6	4	0	1.1075	1.1072	1.3910	334.3	0.19296		0.19512
6	0	4	1.1033	1.1034	1.3963	429.1	0.19295		0.19513
7	1	2	1.0858	1.0856	1.4188	1055.2	0.19295		0.19513
3	3	6	1.0788	1.0784	1.4280	497.2	0.19294		0.19513
6	2	4	1.0637	1.0635	1.4483	630.8	0.19294		0.19512
7	3	2	1.0134	1.0133	1.5202	436.0	0.19294		0.19512
5	1	6	1.0077	1.0074	1.5288	694.5	0.19294		0.19512
8	0	0	0.9982	0.9981	1.5434	164.2	0.19294		0.19511
0	0	8	0.9867	0.9870	1.5614	127.0	0.19294		0.19511
8	2	0	0.9685	0.9683	1.5907	280.8	0.19293		0.19511
6	4	4	0.9657	0.9657	1.5952	431.4	0.19293		0.19511
2	0	8	0.9584	0.9581	1.6074	378.5	0.19293		0.19511
5	3	6	0.9490	0.9489	1.6234	619.2	0.19293		0.19510
2	2	8	0.9319	0.9317	1.6532	384.5	0.19293		0.19510
7	5	2	0.9036	0.9036	1.7050	379.8	0.19293		0.19509
8	4	0	0.8927	0.8927	1.7258	185.4	0.19294		0.19509

8	0	4	0.8909	0.8907	1.7292	241.6	0.19294	0.19509
4	0	8	0.8848	0.8848	1.7411	238.4	0.19293	0.19509
8	2	4	0.8695	0.8694	1.7717	465.9	0.19293	0.19509
4	2	8	0.8638	0.8639	1.7834	675.4	0.19293	0.19509
9	1	2	0.8607	0.8606	1.7898	346.0	0.19293	0.19509
7	1	6	0.8571	0.8570	1.7975	653.5	0.19293	0.19509
6	6	4	0.8494	0.8495	1.8136	213.1	0.19292	0.19509
9	3	2	0.8233	0.8232	1.8713	438.8	0.19293	0.19509
7	3	6	0.8201	0.8201	1.8784	499.0	0.19292	0.19509
8	4	4	0.8135	0.8135	1.8938	430.1	0.19292	0.19509
4	4	8	0.8089	0.8089	1.9045	282.6	0.19292	0.19509
10	0	0	0.7985	0.7985	1.9292	236.4	0.19292	0.19509
6	0	8	0.7927	0.7928	1.9434	226.7	0.19292	0.19509
10	1	1	0.7905	0.7906	1.9488	167.3	0.19292	0.19510

A= 7.9853516 C= 7.8964272

H	K	L	D(O)	D(C)	PEAK	% ERROR	D*(O)	D*(C)
1	0	1	5.6184	5.6148	118.5	0.0638	0.2742	0.2744
2	0	0	3.9921	3.9927	4756.8	0.0139	0.3859	0.3858
1	1	2	3.2331	3.2357	7750.1	0.0803	0.4765	0.4761
2	2	0	2.8215	2.8232	2408.6	0.0606	0.5460	0.5457
2	0	2	2.8077	2.8074	178.1	0.0091	0.5487	0.5488
3	0	1	2.5210	2.5223	572.3	0.0545	0.6111	0.6108
1	0	3	2.4977	2.4998	556.4	0.0871	0.6168	0.6163
3	1	2	2.1267	2.1273	6690.7	0.0298	0.7244	0.7242
2	1	3	2.1176	2.1188	844.7	0.0566	0.7275	0.7271
4	0	0	1.9953	1.9963	695.2	0.0528	0.7721	0.7717
0	0	4	1.9731	1.9741	579.8	0.0534	0.7808	0.7804
4	1	1	1.8794	1.8810	282.4	0.0832	0.8197	0.8190
4	2	0	1.7851	1.7856	1462.4	0.0257	0.8630	0.8628
4	0	2	1.7779	1.7815	90.6	0.2046	0.8665	0.8647
2	0	4	1.7693	1.7696	2255.7	0.0161	0.8707	0.8706
3	3	2	1.6991	1.6990	1971.5	0.0056	0.9067	0.9068
3	2	3	1.6939	1.6946	222.4	0.0470	0.9095	0.9091
2	2	4	1.6177	1.6178	1531.3	0.0068	0.9523	0.9522
1	0	5	1.5489	1.5493	188.3	0.0228	0.9946	0.9944
5	1	2	1.4556	1.4557	2684.6	0.0115	1.0584	1.0583
2	1	5	1.4442	1.4444	107.0	0.0095	1.0667	1.0666
4	4	0	1.4113	1.4116	456.5	0.0240	1.0916	1.0913
4	0	4	1.4033	1.4037	1380.2	0.0273	1.0978	1.0975
3	3	4	1.3607	1.3622	122.0	0.1145	1.1322	1.1309
6	0	0	1.3305	1.3309	359.5	0.0312	1.1579	1.1575
4	2	4	1.3241	1.3242	1800.1	0.0129	1.1635	1.1634
5	3	2	1.2937	1.2939	1223.1	0.0105	1.1908	1.1907
3	2	5	1.2857	1.2859	82.1	0.0095	1.1982	1.1981
1	1	6	1.2817	1.2817	1079.3	0.0042	1.2020	1.2019
6	2	0	1.2623	1.2626	552.5	0.0202	1.2204	1.2202
3	1	6	1.1669	1.1671	1123.0	0.0141	1.3202	1.3200

4	4	4	1.1482	1.1483	352.5	0.0039	1.3417	1.3416
6	4	0	1.1075	1.1074	334.3	0.0136	1.3910	1.3912
6	0	4	1.1033	1.1035	429.1	0.0195	1.3963	1.3960
7	1	2	1.0858	1.0858	1055.2	0.0055	1.4188	1.4189
3	3	6	1.0788	1.0786	497.2	0.0247	1.4280	1.4284
6	2	4	1.0637	1.0637	630.8	0.0047	1.4483	1.4484
7	3	2	1.0134	1.0134	436.0	0.0008	1.5202	1.5202
5	1	6	1.0077	1.0075	694.5	0.0154	1.5288	1.5290
8	0	0	0.9982	0.9982	164.2	0.0010	1.5434	1.5434
0	0	8	0.9867	0.9871	127.0	0.0406	1.5614	1.5608
8	2	0	0.9685	0.9684	280.8	0.0116	1.5907	1.5909
6	4	4	0.9657	0.9658	431.4	0.0051	1.5952	1.5951
2	0	8	0.9584	0.9582	378.5	0.0219	1.6074	1.6078
5	3	6	0.9490	0.9489	619.2	0.0052	1.6234	1.6235
2	2	8	0.9319	0.9318	384.5	0.0123	1.6532	1.6534
7	5	2	0.9036	0.9036	379.8	0.0094	1.7050	1.7048
8	4	0	0.8927	0.8928	185.4	0.0140	1.7258	1.7256
8	0	4	0.8909	0.8908	241.6	0.0151	1.7292	1.7295
4	0	8	0.8848	0.8848	238.4	0.0012	1.7411	1.7411
8	2	4	0.8695	0.8694	465.9	0.0158	1.7717	1.7720
4	2	8	0.8638	0.8639	675.4	0.0022	1.7834	1.7834
9	1	2	0.8607	0.8606	346.0	0.0133	1.7898	1.7900
7	1	6	0.8571	0.8570	653.5	0.0032	1.7975	1.7976
6	6	4	0.8494	0.8495	213.1	0.0054	1.8136	1.8135
9	3	2	0.8233	0.8232	438.8	0.0032	1.8713	1.8714
7	3	6	0.8201	0.8201	499.0	0.0082	1.8784	1.8786
8	4	4	0.8135	0.8135	430.1	0.0010	1.8938	1.8938
4	4	8	0.8089	0.8089	282.6	0.0015	1.9045	1.9045
10	0	0	0.7985	0.7985	236.4	0.0016	1.9292	1.9292
6	0	8	0.7927	0.7928	226.7	0.0121	1.9434	1.9432
10	1	1	0.7905	0.7906	167.3	0.0080	1.9488	1.9486

END OF DATA
*

*U.S.Government Printing Office: 1978 — 757-080/778